



**HAL**  
open science

## Hydrophobic hydration processes. Thermal and chemical denaturation of proteins

E. Fiscaro, C. Compari, A. Braibanti

► **To cite this version:**

E. Fiscaro, C. Compari, A. Braibanti. Hydrophobic hydration processes. Thermal and chemical denaturation of proteins. *Biophysical Chemistry*, 2011, 156 (1), pp.51. 10.1016/j.bpc.2011.02.009 . hal-00750640

**HAL Id: hal-00750640**

**<https://hal.science/hal-00750640>**

Submitted on 12 Nov 2012

**HAL** is a multi-disciplinary open access archive for the deposit and dissemination of scientific research documents, whether they are published or not. The documents may come from teaching and research institutions in France or abroad, or from public or private research centers.

L'archive ouverte pluridisciplinaire **HAL**, est destinée au dépôt et à la diffusion de documents scientifiques de niveau recherche, publiés ou non, émanant des établissements d'enseignement et de recherche français ou étrangers, des laboratoires publics ou privés.

## Accepted Manuscript

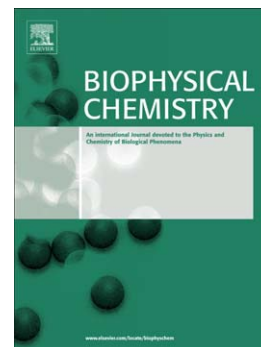
Hydrophobic hydration processes. Thermal and chemical denaturation of proteins

E. Fiscaro, C. Compari, A. Braibanti

PII: S0301-4622(11)00030-5  
DOI: doi: [10.1016/j.bpc.2011.02.009](https://doi.org/10.1016/j.bpc.2011.02.009)  
Reference: BIOCHE 5483

To appear in: *Biophysical Chemistry*

Received date: 2 February 2011  
Revised date: 21 February 2011  
Accepted date: 21 February 2011



Please cite this article as: E. Fiscaro, C. Compari, A. Braibanti, Hydrophobic hydration processes. Thermal and chemical denaturation of proteins, *Biophysical Chemistry* (2011), doi: [10.1016/j.bpc.2011.02.009](https://doi.org/10.1016/j.bpc.2011.02.009)

This is a PDF file of an unedited manuscript that has been accepted for publication. As a service to our customers we are providing this early version of the manuscript. The manuscript will undergo copyediting, typesetting, and review of the resulting proof before it is published in its final form. Please note that during the production process errors may be discovered which could affect the content, and all legal disclaimers that apply to the journal pertain.

**HYDROPHOBIC HYDRATION PROCESSES.  
THERMAL AND CHEMICAL DENATURATION OF PROTEINS**

*E. Fiscaro, C. Compari, and A. Braibanti*

*Department of Pharmacological, Biological and Applied Chem. Sciences, Physical Chemistry Section,  
University of Parma, I-43100 Parma, Italy. Fax:39 0521 905026 e-mail: fiscaro@unipr.it*

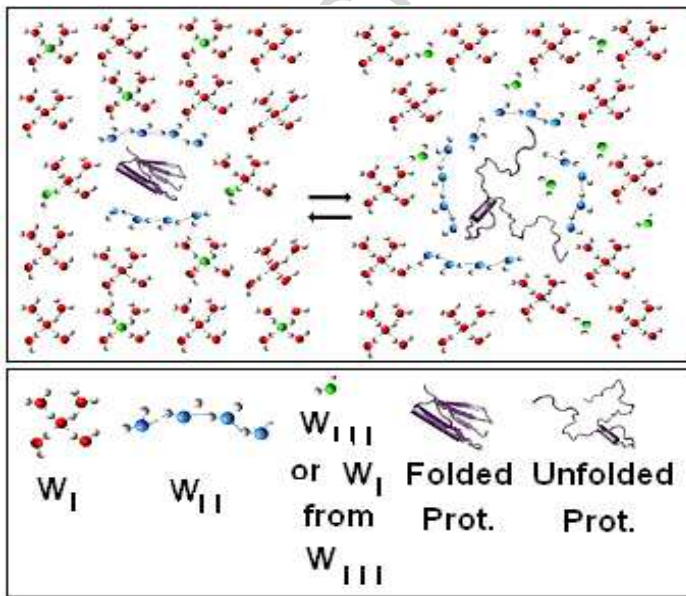
**Abstract**

The hydrophobic hydration processes have been analysed under the light of a mixture model of water that is assumed to be composed by clusters  $(W_5)_I$ , clusters  $(W_4)_{II}$  and free water molecules  $W_{III}$ . The hydrophobic hydration processes can be subdivided into two Classes A and B. In the processes of Class A, the transformation **A** ( $-\xi_w W_I \rightarrow \xi_w W_{II} + \xi_w W_{III} + \text{cavity}$ ) takes place, with expulsion from the bulk of  $\xi_w$  water molecules  $W_{III}$ , whereas in the processes of Class B the opposite transformation **B** ( $-\xi_w W_{III} - \xi_w W_{II} \rightarrow \xi_w W_I - \text{cavity}$ ) takes place, with condensation into the bulk of  $\xi_w$  water molecules  $W_{III}$ . The *thermal equivalent dilution (TED)* principle is exploited to determine the number  $\xi_w$ . The denaturation (unfolding) process belongs to Class A whereas folding (or renaturation) belongs to Class B. The enthalpy  $\Delta H_{den}$  and entropy  $\Delta S_{den}$  functions can be disaggregated in thermal and motive components,  $\Delta H_{den} = \Delta H_{therm} + \Delta H_{mot}$ , and  $\Delta S_{den} = \Delta S_{therm} + \Delta S_{mot}$ , respectively. The terms  $\Delta H_{therm}$  and  $\Delta S_{therm}$  are related to phase change of water molecules  $W_{III}$ , and give no contribution to free energy ( $\Delta G_{therm}=0$ ). The motive functions refer to the process of cavity formation (Class A) or cavity reduction (Class B), respectively and are the only contributors to free energy  $\Delta G_{mot}$ . The folded native protein is thermodynamically favoured ( $\Delta G_{fold} \equiv \Delta G_{mot} < 0$ ) because of the outstanding contribution of the positive entropy term for cavity reduction,  $\Delta S_{red} \gg 0$ . The native protein can be brought to a stable denatured state ( $\Delta G_{den} \equiv \Delta G_{mot} < 0$ ) by coupled reactions. Processes of protonation coupled to denaturation have been identified. In thermal denaturation by calorimetry, however, is the heat gradually supplied to the system that yields a change of phase of water  $W_{III}$ , with creation of cavity and negative entropy production,  $\Delta S_{for} \ll 0$ . The negative entropy change reduces and at last neutralises the positive entropy of folding. In molecular terms, this means the gradual disruption by cavity formation of the entropy-driven hydrophobic bonds that had been keeping the chains folded in the native protein. The action of the chemical denaturants is similar to that of heat, by modulating the equilibrium between  $W_I$ ,  $W_{II}$ , and  $W_{III}$  toward cavity formation and negative entropy production. The salting-in effect produced by denaturants has been recognised as a hydrophobic hydration process belonging to Class A with cavity formation, whereas the salting-out effect produced by stabilisers belongs to Class B with cavity reduction.

Some algorithms of denaturation thermodynamics are presented in the Appendices.

**Graphical abstract**

## Graphical Abstract



## Research Highlights

The molecular model (FCB model) of water, based on tree forms of water,  $W_I$ ,  $W_{II}$ , and  $W_{III}$ , is suited to interpret all the Hydrophobic Hydration Processes. These processes can be subdivided into two Classes A and B. In the processes of Class A, the transformation **A**( $-\xi_w W_I \rightarrow \xi_w W_{II} + \xi_w W_{III} + \text{cavity}$ ) takes place, with expulsion from the bulk of  $\xi_w$  water molecules  $W_{III}$ , whereas in the processes of Class B the opposite transformation **B**( $-\xi_w W_{III} - \xi_w W_{II} \rightarrow \xi_w W_I - \text{cavity}$ ) takes place, with condensation into the bulk of  $\xi_w$  water molecules  $W_{III}$ .

The enthalpy  $\Delta H_{app}$  and entropy  $\Delta S_{app}$  functions can be disaggregated in thermal and motive components,  $\Delta H_{app} = \Delta H_{therm} + \Delta H_{mot}$ , and  $\Delta S_{app} = \Delta S_{therm} + \Delta S_{mot}$ , respectively. The terms  $\Delta H_{therm}$  and  $\Delta S_{therm}$  are related to phase change of water molecules  $W_{III}$ , and give no contribution to free energy ( $\Delta G_{therm}=0$ ).

We have now applied the FBC model to the analysis of protein denaturation, either thermal or chemical. In thermal denaturation, the heat gradually supplied to the system yields a change of phase of water  $W_{III}$ , with creation of cavity and negative entropy production,  $\Delta S_{red} = (\Delta S_{mot} - \Delta S_0^{(\xi_w=0)}) \ll 0$ , with disruption by cavity formation of the entropy-driven hydrophobic bonds that had been keeping the chains folded in the native protein.

In chemical denaturation, the denaturants and stabilizers modulate the equilibrium among the various forms of water,  $W_I$ ,  $W_{II}$ , and  $W_{III}$  toward cavity formation (Class A, denaturants) or toward cavity reduction (Class B, stabilizers). The same template mechanism explains the phenomena of “salting in” (belonging to Class A) and “salting out” (belonging to Class B).

**Keywords:** water clusters, cavity formation, cavity reduction, thermal enthalpy, thermal entropy, motive free-energy

## 1. Introduction<sup>1</sup>

We have studied [1-3] the thermodynamics of the solubility in water of non-polar gases in comparison with the thermodynamics of micelle formation in water. The analysis has been pursued on the basis of a structure model (FCB model) for water. The FCB model assigns to water three structures consisting of clusters ( $W_5$ )<sub>I</sub>, clusters ( $W_4$ )<sub>II</sub> and free water molecules  $W_{III}$ , respectively. Release of  $\xi_w$  water molecules  $W_{III}$  from  $W_I$  produces water  $W_{II}$  and creates a cavity to host the solute molecule. In the solution,  $W_I$  (low density) forms the bulk,  $W_{II}$  (high density) forms a sheath around the solute molecule and  $W_{III}$  are free water molecules.

The FCB model has allowed the interpretation of every hydrophobic hydration process [4] by considering that each process, although apparently different from one another, refers to a unique transformation of water clusters, direct or inverse.

The hydrophobic hydration processes can be subdivided into two Classes A and B ( Fig.1). In the processes of Class A, the transformation **A**( $-\xi_w W_I \rightarrow \xi_w W_{II} + \xi_w W_{III} + \text{cavity}$ ) takes place, with expulsion from the bulk of  $\xi_w$  water molecules  $W_{III}$ , whereas in the processes of Class B the opposite transformation **B**( $-\xi_w W_{III} - \xi_w W_{II} \rightarrow \xi_w W_I - \text{cavity}$ ) takes place, with condensation into the bulk of  $\xi_w$  water molecules  $W_{III}$ , (“-cavity“ is equivalent to cavity reduction) .

The number  $\xi_w$  depends on the size of the reactant molecules. The value of  $\xi_w$  has been calculated from the slope  $\Delta C_p$  of the plot  $\Delta H_{app} = f(T)$  by applying the principle of *thermal*

Fig. 1. A unique reaction, involving water, either direct (left, Class A)) or inverse (right, Class B) takes place in every hydrophobic hydration process:

- Unfolding (Class A): transformation **A**( $-\xi_w W_I \rightarrow \xi_w W_{II} + \xi_w W_{III} + \text{cavity}$ ), with melting of  $\xi_w$  water molecules  $W_{III}$ .
- Folding (Class B): transformation **B**( $-\xi_w W_{III} - \xi_w W_{II} \rightarrow \xi_w W_I - \text{cavity}$ ), with condensation of  $\xi_w$  water molecules  $W_{III}$ .

Cavity expansion or reduction ( $\pm \Delta W_I$ , in grey) is proportional to  $\xi_w$ . Note, please, that the sum of white and grey areas at the bottom equals the sum of the separated white areas at the top.

*equivalent dilution (TED)* [4,14] from the equality

$$\Delta C_p = \pm \xi_w C_{p,w} \quad (1)$$

where  $C_{p,w}=75.36 \text{ J}\cdot\text{K}^{-1}\text{mol}^{-1}$  is the isobaric heat capacity of liquid water. The sign + in Eq. (1) holds for Class A and the sign – for Class B. A large value of  $\Delta C_p$  has been recognised as a typical property of all the hydrophobic hydration processes [5-8]. Moreover  $\Delta C_p$ , and hence  $\xi_w$ , has been found to be linearly related to the length of the chain [5] or resulting as the summation of group contributions [7]. The ranges of  $\xi_w$  are different for small or large molecules, but the unitary (*i.e.* for  $\xi_w =1$ ) quantities for enthalpy and entropy are practically equal, respectively, independently from the total molecular size.

## 2. Thermal and Motive Functions

<sup>1</sup> For symbols see **Glossary** before **References**

Some years ago, R. Lumry [9] has raised some doubts whether the thermodynamic data can be user-friendly if applied to isothermal processes. He thinks that enthalpy, internal energy, entropy and volume data are generally suspect since rarely have they been analysed so as to take the two species of water into account. He thinks also that the statements by Benzinger [10] that there might exist some hidden part of enthalpy and entropy not contributing to the free energy add more doubts to the validity of the thermodynamic functions as representative of the chemical reactions. Another word of caution about the splitting of  $\Delta G$  into enthalpic and entropic contributions and its temperature dependence on the basis of oversimplified (inadequate) models of the protein interaction is launched by Winzor and Jackson [11]. The main possible reactions that, according to these authors, are linked to the proper protein transformations, could be isomerisation reactions, proton-base equilibria, or protein-ligand interactions. Another question raised by Lumry [12,13] concerns the thermodynamic functions for denaturation, enthalpy  $\Delta H_{den}$  and entropy  $\Delta S_{den}$ , that, according to Lumry, should be subdivided into two parts, motive (or work) and thermal (or compensative) functions.

We think, however, that the criticisms of Lumry, Winzor and Jackson should not be applicable to our treatment, because the model that we assume takes into account actually two types of water clusters, *i.e.*  $(W_5)_I$  and  $(W_4)_{II}$ , as required by Lumry [9], together with free water molecules  $W_{III}$ . Moreover the problem of integration of the two thermal functions of Benzinger have been solved by us. As far as side reactions are concerned, the main side reaction that we have taken into account in micelle formation and in solubility of non-polar substances is just the change of phase of water  $W_{III}$  that can either melt by leaving water  $W_I$  or condense into  $W_I$ . The change of phase of water  $W_{III}$  have been shown to correspond exclusively to the thermal (or compensative) components of the thermodynamic functions suggested by Lumry. These thermal components can be identified as the hidden parts indicated by Benzinger. On the other hand, the motive components of Lumry can be associated to the process of cavity formation. Moreover, coupled protonation equilibria will be considered in the study of denaturation.

We now want to analyse whether the thermodynamic functions of protein denaturation and protein folding, calculated from the experimental data, conform to the same model FCB as the thermodynamic functions of Class A and Class B, respectively and how much the thermodynamic functions, free energy  $\Delta G_{den}$ , enthalpy  $\Delta H_{den}$  and entropy  $\Delta S_{den}$ , are in qualitative or even quantitative agreement with the results obtained with the other hydrophobic hydration processes of

Fig. 2. Examples of free energy plots  $(-\Delta G^\circ)/RT = \ln K = f(1/T)$  in hydrophobic hydration processes.

both Classes.

The subdivision in Classes A and B has been done by analysing the type of curve presented in the free energy plot  $(-\Delta G^\circ)/RT = \ln K = f(1/T)$  by any hydrophobic hydration process<sup>2</sup>. The plots of the processes of Class A (Fig.2, A) present invariably a minimum whereas the processes of Class B (Fig.2, B) show curves with a maximum. The type of curvature depends in particular on the type of

Fig. 3. Mechanism of unfolding of a protein.

cavity-change in the solvent, with cavity formation in Class A and cavity reduction in Class B.

A process analogous to that of gas solubility and opposite to that of micelle formation can be proposed for denaturation (Fig. 3). The hydrophobic chains previously associated in the folded protein, detach from each other and distend into the bulk of the liquid. In order to do so, they need

<sup>2</sup> Relationships between thermodynamic functions and partition function can be found in Appendix A from Eq. (A.6) to Eq. (A.16)

more room and in fact a larger cavity is formed by releasing from the bulk a number  $\xi_w$  of free water molecules  $W_{III}$ . At the same time, clusters  $(W_5)_I$  are transformed into clusters  $(W_4)_{II}$ . The equations of the equilibria involved in protein denaturation and the consequent thermodynamic relationships are developed in Appendix A.

We have identified as a member of Class A the process of denaturation (unfolding of the chains) and as a member of Class B the process of protein structuring (folding of the chains or renaturation, with hydrophobic bonding). The applications of this model would help us to find a rational explanation of the mechanism of both thermal and chemical denaturation of proteins.

The equilibrium denatured/native is ruled by a dissociation constant  $K_{den}$ . The free energy function

$$(-\Delta G_{den}^{\theta})/RT = \ln K_{den} = f(1/T) \quad (2)$$

is represented, as well as any other process of Class A, by a curve with a minimum. This shape of the curve means that the tangent to the curve of Eq. (2), given by van't Hoff equation

$$\partial(\ln K_{den})/\partial(1/T) = -\Delta H_{den}/R \quad (3)$$

is changing from a negative slope at the left of the minimum to a positive slope at the right of the minimum. By calculating the derivative at any temperature of the interval, by changing sign, and by plotting  $\Delta H_{den}$  against  $T$ , we obtain, for every process of Class A, a linear expression

$$\Delta H_{den} = \Delta H_{(0)} + \Delta C_p T \quad (4)$$

with intercept  $\Delta H_{(0)} < 0$  and slope  $\Delta C_p > 0$ . By applying *TED* [4, 14] we can set

$$\Delta C_p = \xi_w C_{p,w} \quad (5)$$

where  $C_{p,w}$  is the isobaric heat capacity of liquid water. Both intercept  $\Delta H_{(0)}$  and slope  $\Delta C_p$  are different for each compound of any type of process because they both are linear functions of the same  $\xi_w$ .

Eq. (4) is suited to distinguish the two components, motive and thermal, respectively, that form the thermodynamic functions according to the suggestions of Lumry [12, 13]. The denaturation enthalpy  $\Delta H_{den}$ , in fact, can be seen as composed of two parts, thermal part  $\Delta H_{therm}$  and motive part  $\Delta H_{mot}$ :

$$\Delta H_{den} = \Delta H_{mot} + \Delta H_{therm} \quad (6)$$

with  $\Delta H_{mot} \equiv \Delta H_{(0)}$  (*i.e.* the intercept  $\Delta H_{(0)}$  of Eq. (4)). The thermal part  $\Delta H_{therm}$ , by comparison with Eq. (4) and Eq. (5),

$$\Delta H_{therm} = +\xi_w C_{p,w} T \quad (7)$$

results to be attributable exclusively to the thermal energy gained by  $\xi_w$  water molecules  $W_{III}$  removed from the bulk of the solvent and moving in the interstices.

The motive (or work) part  $\Delta H_{mot}$  is composed of two terms

$$\Delta H_{mot} = (\Delta H_0^{(\xi_w=0)} + \Delta H_{for}) = (\Delta H_0^{(\xi_w=0)} + \xi_w \cdot \Delta h_{for}) \quad (8)$$



thus showing that  $\Delta H_{mot}$  is independent from the temperature but depends on factors attaining strictly to the cavity formation of size  $\xi_w$  ( $\Delta H_{for}$ ) and to the affinity or repulsion between hydrophobic moieties ( $\Delta H_0^{(\xi_w=0)}$ ).

By plotting the denaturation entropy against  $\ln T$ , we obtain a straight line

$$\Delta S_{den} = \Delta S_{(0)} + \Delta C_p \ln T \quad (9)$$

where the slope  $\Delta C_p$  (cf. Eq. (5)) is exactly the same obtained from the plot  $\Delta H_{den} = f(T)$  for the same compound. It is thus possible to represent the entropy as composed of two parts, thermal part  $\Delta S_{therm}$  and motive part  $\Delta S_{mot}$

$$\Delta S_{den} = \Delta S_{mot} + \Delta S_{therm} \quad (10)$$

with  $\Delta S_{mot} \equiv \Delta S_{(0)}$  (i.e. the intercept  $\Delta S_{(0)}$  of Eq. (9)). The thermal entropy  $\Delta S_{therm}$  is identified as

$$\Delta S_{therm} = + \xi_w C_{p,w} \ln T \quad (11)$$

that is attributable exclusively to the thermal entropy gained, starting from the resting state of the condensed structure (at  $\ln T = 0$ ), by  $\xi_w$  water molecules  $W_{III}$  removed from the bulk of the solvent and moving in the interstices. The motive entropy, composed by two terms,

$$\Delta S_{mot} = (\Delta S_0^{(\xi_w=0)} + \Delta S_{for}) = (\Delta S_0^{(\xi_w=0)} + \xi_w \cdot \Delta S_{for}) \quad (12)$$

is independent from the temperature:  $\Delta S_{for}$  is related to the process of cavity formation and  $\Delta S_0^{(\xi_w=0)}$  refers to some configurational (concentration) change of the macromolecule as a whole.

The thermal enthalpy of Eq. (7) and the thermal entropy of Eq. (11) are related each other by the relationship

$$\Delta H_{therm}/T = \Delta S_{therm} \quad (13)$$

whereby the reaction of water molecules  $W_{III}$ , that are moving from the resting structured state to the disordered fluid state, shows a behaviour similar to a phase change, like a melting process. The heat supplied to the melting molecules is transformed into kinetic energy of the same molecules in the fluid phase. The only difference is that, while the melting process takes place, under constant pressure, at a definite constant temperature, Eq. (13) is valid at any temperature we perform the experiment. Another point that deserves attention is the correspondence of the thermal parts of enthalpy ( $+\xi_w C_{p,w} T$ ) and entropy ( $\xi_w C_{p,w} \ln T$ ) with the two integrals proposed by Benzinger [10],  $\Delta S^\circ_T = \int \Delta C_p dT$  and  $\Delta \Gamma^\circ_T = \int (\Delta C_p / T) dT$ , respectively. The importance of these hidden functions in thermodynamics of protein unfolding had been underlined by Benzinger himself.

### 3. Denaturation Free Energy as a Function of Temperature and pH

Free energy data for the denaturation at different temperatures has been reported by R. Lumry *et al.* [12]. The proteins examined by them were chymotrypsinogen A (CGN), its dimethionine sulfoxide derivative (DMSCGN), diphenyl-carbamyl- $\alpha$ -chymotrypsin (DPC- $\alpha$ -CT), and

Fig. 4. Cumulative curve of  $\log K_{den}$  for DMSCGN (dimethionine sulfoxide derivative of chymotrypsinogen) with all the branches displaced to pH=2.

Parallel displacement to pH = 0 brings the whole curve in the positive range of  $\log K_{den}$  ( $\Delta G_{den} < 0$ ) where the denatured state is stable.

ribonuclease (RNase). The advancement of the reaction was followed spectrophotometrically. Particular care has been devoted by the Authors to the reversibility of the transitions. The following questions have been discussed by them: (1) Because of the arbitrariness introduced by the choice of the mathematical interpolation, can one obtain accurate heat-capacity information about unfolding reactions of proteins from thermal equilibrium studies? (2) What empirical equation best describes quantitatively the thermodynamic information about unfolding transitions? Analysis of data of conformational transitions is simple only if the transitions can be approximated by a two state model. Aggregation is strongly dependent on temperature, pH, protein and salt concentration. A special problem has arisen in the determination of the spectrophotometric baseline. They conclude that the errors generated by the uncertainty in the baseline at the foot and top of two different transition curves are largest and only values of  $\Delta H_{den}$  and  $T$  near the middle of the transitions (around  $\Delta G=0$ ) present a high degree of consistency among the proteins of the chymotrypsinogen family. The result of RNase were obtained with considerable accuracy. The Authors have verified that the dependence of  $\Delta H_{den}$  upon pH does not involve  $\Delta C_p$  and therefore the data obtained at pH 2.8 or other pH levels could be readily corrected to pH 2. The variations of the free energy functions with pH are examined in detail in Appendix B. There is also shown how it is possible to construct for each protein, a unique cumulative curve for free energy (and of course for  $\log K_{den}$ ) starting from sets of experimental values obtained at different pH levels. An example of curve of  $\log K_{den}$  for DMSCGN as normalised to pH=2 (Fig. 4) shows that the values of  $\log K_{den}$  lay in the range of the negative values ( $\log K_{den} < 0$ ,  $\Delta G_{den} > 0$ ). The denatured state is, therefore, thermodynamically unstable. The curve at pH=2, however, can be displaced parallel to itself by changing pH from pH=2 to pH= 0. The cumulative curve moves thus to the field of the positive values ( $\log K_{den} > 0$ ,  $\Delta G_{den} < 0$ ), thus showing that the denatured state has become thermodynamically favoured. This explains the action of proton as denaturant. Actually we have used the normalised cumulative sets obtained from the original data of Lumry [12] for the four proteins to calculate  $\Delta H_{den}$  and  $\Delta S_{den}$ . The equations representing the cumulative curves are reported in Table 1.

Table 1. Equations representing the cumulative curves at pH=2.

The values of  $\Delta H_{den}$  for different proteins, obtained from the curves  $\log K_{den}$  as the function of  $(1/T)$ , plotted against  $T$ , produce linear plots, as expected (Fig. 5). The values of  $\Delta S_{den}$  have been calculated by the Helmholtz-Gibbs equation and then plotted against  $\ln T$ , thus obtaining linear plots, with the same slopes  $\Delta C_p = \xi_w C_{pw}$  found for enthalpy (Fig. 6). The equations corresponding to each compound are reported in Table 2. The values of the numbers  $\xi_w(S)$  calculated from the entropy plot are practically equal to those  $\xi_w(H)$  obtained from the enthalpy plots. The values of  $\xi_w$  obtained are reasonable because they are much larger than those found in the solubility of non-polar substances and in micelle formation but are as large as those found in other proteins, as calculated either by equilibrium or calorimetric determinations.

The values of the motive functions (cf. Eq. (8)) can be, on their turn, disgregated in two terms, the first referring to the inter-chain interaction and the second to the process of cavity formation (Table 3). The value for enthalpy  $\Delta h_{for} = -22.5 \text{ kJ}\cdot\text{mol}^{-1}\cdot\xi_w^{-1}$  is the unitary enthalpy change for the transformation from clusters  $(W_5)_I$  to clusters  $(W_4)_{II}$  with cavity formation, for each water molecule

Fig. 5. Example of plot  $\Delta H_{den} = f(T)$  (DMSCGN, dimethionine sulfoxide derivative of chymotrypsinogen).

$W_{III}$  released. The partial reaction of cavity formation is, therefore, exothermic. The unitary enthalpy is very close to  $\Delta h_{for} = -21.6 \text{ kJ}\cdot\text{mol}^{-1}\cdot\xi_w^{-1}$  found in the solubility of non-polar substances for the same process and, with change of sign, to  $\Delta h_{red} = +23.2 \text{ kJ}\cdot\text{mol}^{-1}\cdot\xi_w^{-1}$  for the opposite process of micelle formation with cavity reduction. For the entropy of cavity formation, we find the

Table 2. Denaturation Enthalpy and Entropy as sum of motive and thermal components.

unitary value  $\Delta S_{for} = -424.2 \text{ J}\cdot\text{K}^{-1}\cdot\text{mol}^{-1}\cdot\xi_w^{-1}$  indicating the loss of entropy for cavity formation for each water molecule  $W_{III}$  released. This can be compared with  $\Delta S_{for} = -445 \text{ J}\cdot\text{K}^{-1}\cdot\text{mol}^{-1}\cdot\xi_w^{-1}$

Fig. 6. Example of entropy plot. (DMSCGN, dimethionine sulfoxide derivative of chymotrypsinogen).

found for the same process in the solubilisation of non polar substances. It is also very similar, with change of sign, to the opposite process of cavity reduction in micelle formation  $\Delta S_{red} = +433 \text{ J}\cdot\text{K}^{-1}\cdot\text{mol}^{-1}\cdot\xi_w^{-1}$ .

Table 3. Motive Functions: cavity formation and intra-chain interactions.

On the whole, we can assume that these coincidences of quantities are not casual and strongly support the idea that the molecular model working for the solubilisation of non polar compounds (Class A) is valid also for the denaturation of proteins. Analogously, the model working for micelle formation (Class B) is valid for the process of protein folding or protein renaturation.

#### 4. Denaturation: Entropy-Opposed Process

The distinction between motive and thermal parts of the thermodynamic functions can be exploited to separate the contributions of the real chemical reaction of cavity formation or reduction from the contributions of the change of phase of water  $W_{III}$ . The latter contribution coincides with the thermal part both in Eq. (6) and Eq. (10). Following Lumry [12, 13], we consider, on the grounds of Eq. (13), that the motive parts  $\Delta H_{mot}$  and  $\Delta S_{mot}$  only contribute to the motive free energy  $\Delta G_{mot}$ , thus obtaining a Helmholtz-Gibbs equation

$$\Delta G_{mot} = \Delta H_{mot} - T \Delta S_{mot} \quad (14)$$

In the denaturation of proteins, therefore, the separation of both enthalpy and entropy into thermal and motive parts is possible. The motive components have been calculated and reported in Table 4. An example is presented in Fig. 7. The diagram demonstrates that the denaturation process.

Fig. 7. Motive parts of enthalpy, entropy and free energy for protein denaturation ( $\Delta H_{mot} = -2823 \text{ kJ}\cdot\text{mol}^{-1}$ ).

is thermodynamically disfavoured due to the outstanding contribution of the negative entropy change ( $\Delta S_{for} \ll 0$ ) for cavity formation. In contrast, by attributing to the process of folding the same

values of the thermodynamic functions with reversed signs, we can see (simply by changing sign to the ordinates of the diagram in Fig. 7) that the native folded state is thermodynamically favoured because entropy-driven by the prominent contribution of the positive entropy change ( $\Delta S_{red} \gg 0$ ) of cavity reduction. The folding of the protein would seem to correspond to a decrease in entropy, but is the positive entropy production of cavity reduction that becomes the prominent contributor to the negative motive free energy  $\Delta G_{fold}$  ( $\Delta G_{fold} \equiv \Delta G_{mot}$ ). In fact, in the process of folding, notwithstanding the protein itself is obviously more ordered in the folded state than in the unfolded one, the entropy increases, the increase deriving from the development of the reaction  $\mathbf{B}(-\xi_w W_{III} - \xi_w W_{II} \rightarrow \xi_w W_I - \text{cavity})$  toward cavity reduction, with condensation into  $W_I$  of  $\xi_w$  water molecules  $W_{III}$  and production of entropy for cavity reduction (cf.  $\langle \Delta s_{red} \rangle_B = +432 \pm 4 \text{ J}\cdot\text{K}^{-1}\cdot\text{mol}^{-1}\cdot\xi_w^{-1}$ , with  $\Delta S_{red} \gg 0$ ).

Table 4. Motive parts of the thermodynamic functions for protein denaturation.

The amounts of the thermodynamic functions reported in Table 4 look very high, but this is due to the large number of interactions involved in the transformation. As a matter of fact, we must remember that the values of the thermodynamic functions associated to each unit of water  $W_{III}$  calculated either in large or small molecules are almost coincident. This fact indicates that the same type of reaction referred to one unit  $W_{III}$  is taking place both in large and small molecules.

## 5. Coupled Protonation Equilibria

The denaturation enthalpy  $\Delta H_{den}$  for every protein can then be represented by the general equation

$$\Delta H_{den} = (\Delta H_0^{\xi_w=0} + \Delta H_{for}) + \Delta H_{therm} = (+205.05 - 22.5 \xi_w) + \xi_w C_{p,w} T \quad (15)$$

where the isobaric heat capacity of water is  $C_{p,w} = 0.07536 \text{ kJ}\cdot\text{K}^{-1}\cdot\text{mol}^{-1}$ .

The denaturation entropy can be represented by an equation that corresponds term by term to Eq. (15), that is

$$\Delta S_{den} = (\Delta S_0^{\xi_w=0} + \Delta S_{for}) + \Delta S_{therm} = (-59.7 - 424.2 \xi_w) + \xi_w C_{p,w} \ln T \quad (16)$$

where  $C_{p,w} = 75.36 \text{ J}\cdot\text{K}^{-1}\cdot\text{mol}^{-1}$  and  $\xi_w$  indicates again the number of water molecules of type  $W_{III}$ ,  $\Delta S_{for} = \xi_w \Delta s_{for} < 0$  is the entropy change for cavity formation and the term  $\Delta S_{therm} = \xi_w C_{p,w} \ln T$  is the thermal entropy gained by  $\xi_w$  water molecules  $W_{III}$ .

The expressions for  $\Delta H_{den}$  in Eq. (15) and for  $\Delta S_{den}$  in Eq. (16) both repeat the paradigm of Class A of the hydrophobic hydration processes. By calculating enthalpy and entropy by Eq. (15) and Eq. (16), respectively, the total free energy change for cavity formation for the four compounds examined can be obtained. The curves present the expected shape (Fig. 8) with a maximum falling within the experimental range. The curves refer to the process of cavity formation and they can be

Fig. 8. Calculated free energies in protein denaturations.

used to calculate  $\log K_{for}$  of cavity formation.

In order to give an answer to the objections of R. Lumry[9] and D.J. Winzor and C. M Jackson [11], we have considered here a sort of hydration equilibrium. In the protonation of carboxylic acids in aqueous solution, we have shown that not only the hydration reaction but also the actual combination of proton with the base contributes to the energetics of the reaction by a specific detectable protonation constant. We have, therefore, calculated the residual constant  $\Delta\log K_x$  by calculating the difference between the constant  $\log K_{den}$  of the experimental cumulative curve for each protein and the constant  $\log K_{for}$  calculated by means of Eq. (15) and Eq. (16).

$$\log K_{den} = \log K_{for} + \Delta\log K_x \quad (17)$$

Then,  $\Delta\log K_x$  has been plotted against  $(1/T)$  thus obtaining linear van't Hoff plots (Fig. 9). The existence of linear plots  $\Delta\log K_x = f(1/T)$  of the residual constant demonstrates that, coupled to the denaturation equilibrium between native and denatured form and to the dehydration reaction, there is also a protonation equilibrium that is active on three sites<sup>3</sup> at the very moment of denaturation.

Fig. 9. Van't Hoff plot of  $\Delta\log K$  for RNase.

Eq. (17) can be rewritten

$$\log K_{den} = \log K_{for} + \log K_{prot} \quad (18)$$

From slope and intercept of the lines in the van't Hoff plot, the values of  $\Delta H_{prot}$  and  $\Delta S_{prot}$  have been calculated. The thermodynamic functions relative to each one-site reaction are obtained by dividing by three. All the values are reported in Table 5.

Table 5. Thermodynamic functions calculated from the van't Hoff plot of  $\Delta\log K$  (\*)

(\*) Division by 3 (cfr. power  $\langle x \rangle = 3.04 \pm 0.08$  in Table B.1) to refer to a one-site reaction

## 6. Thermodynamic Functions by Calorimetric Determinations

The denaturation of proteins can be studied by calorimetry also. We can demonstrate that the enthalpy determined calorimetrically follows the same rules, as that found from equilibrium determinations.

The DSC microcalorimeter has been used by several Authors [15-19] to study the equilibrium between native and denatured conformations of macromolecules. The first set of data that we have analysed under the light of the FCB model is that reported by Privalov[16]. We have measured the peaks of the calorimetric traces obtained for HEW lysozyme under different pH and determined either by isothermal (IC) or differential scanning (DSC) calorimetry. The number of water

Fig. 10. Dependence of enthalpy on the temperature  $T_{den}$  for a wild type of lysozyme from bacteriophage T4 and its T157A mutant.

<sup>3</sup> The factor 3 has been calculated from the displacements of the curves as the function of pH (cf. Table B.1)

molecules that we have calculated from the slope of the line is  $\xi_w = 88.9$ . Other sets of calorimetric data concerning various types of lysozyme have been obtained by J. M. Sturtevant and reported [20].

Typical plots of denaturation enthalpies against  $T_{den}$  for T4 lysozyme are presented in Fig.10. Several different batches of proteins were used in each case and this could be the cause of the considerable scattering in the data. The temperature of denaturation  $T_{den}$  was varied by varying the pH over the range 1.8 to 3.1. The different mutants produce lines with different slopes corresponding to  $\xi_w = 122$  for wild T4 lysozyme,  $\xi_w = 131.4$  for Thr157Ala, and  $\xi_w = 139.8$  for Arg96His, respectively.

Table 6. Dehydration numbers,  $\xi_w$  from calorimetry in different types of lysozyme.

(!)  $T_{ad}$  is the temperature where  $\Delta H_{app} = 0$  (adiabatic)

The dehydration numbers obtained from thermal denaturation enthalpy for different types of lysozyme are reported in Table 6. The changes in the number of water molecules,  $\xi_w$  are coherent with the molecular features of the types of lysozyme. The variation between HEW and T4 lysozyme is related to the size of the molecules. The wild T4 lysozyme has a sequence of 164 residues against 126 of HEW lysozyme. The molecular weight of T4 Lysozyme is 18,700 Da against 14,100 Da for HEW lysozyme. On the whole, the molecule of T4 lysozyme is larger than the molecule of HEW lysozyme and very likely presents a number of hydrophobic residues which is roughly proportional to the molecular size. The changes of  $\xi_w$  between wild T4 lysozyme and its mutants are justified by the increased hydrophobic character of the substituents. Ala is more hydrophobic than Thr and His more hydrophobic than Arg, respectively

The values of the extrapolated enthalpy  $\Delta H_{mot}$  obtained from calorimetry plotted against  $\xi_w$  yield values  $\Delta h_{for} = -21.13 \text{ kJ}\cdot\text{mol}^{-1}\cdot\xi_w^{-1}$  and  $\Delta H_0^{(n_w=0)}$  that are practically equal to those obtained

Table 7. Enthalpy and entropy functions in corresponding processes(°).

(°)  $\Delta h_w$  and  $\Delta s_w$  indicate general unitary thermodynamic functions of either Class, *i.e.*  $\Delta h_w$  and  $\Delta s_w$  indicate  $\Delta h_{for}$  and  $\Delta s_{for}$ , respectively, in Class A and  $\Delta h_{red}$  and  $\Delta s_{red}$ , respectively, in Class B.

by van't Hoff equation (Table 7). They conform to the values obtained (with sign reversed) in micelle formation and protein folding, although they have been obtained in experiments of completely different types.

## 7. Calorimetric Denaturation and Cavity Formation

In order to find a reasonable explanation of the mechanism of thermal denaturation, we presume that the folded native protein had been formed through a process of hydrophobic association analogous to that of micelle formation, with an outstanding positive entropic contribution. We recall that the hydrophobic bonding is driven by the positive entropy change,  $\Delta S_{red} \gg 0$  produced as the consequence of the condensation of  $\xi_w$  water molecules  $W_{III}$  into water  $W_I$ , with cavity reduction  $\mathbf{B}(\xi_w W_{III} + \xi_w W_{II} \rightarrow \xi_w W_I - \text{cavity})$ . The folded native protein can be, therefore, assigned unitary values of the thermodynamic stepwise functions equal to those of the denaturation steps, with sign reversed.  $W_{III}$  is that part of the system that is giving rise to a change of phase, from structured to fluid state. When the heat supply starts, the heat moves a molecule of water  $W_{III}$  displacing the equilibrium toward the fluid state. The whole process (Table 8) takes place through three steps:

1) **Start:** the heat supplied to the system generates melting of some water  $W_{III}$ , creating the cavity. In fact, the creation of the cavity ( $dV_{for}>0$ ) produces negative entropy ( $dS_{for}<0$ ), thus beginning to cancel the positive entropic contribution of protein folding ( $\Delta S_{red} + dS_{for}$ ).

2) **Scanning:** the process of heat supply continues (integration) until the total entropy change for cavity formation,  $\Delta S_{for}<<0$  completely compensates for the entropy change  $\Delta S_{red}>>0$  of the protein folding

3) **Final:** at this stage ( $\Delta S_{red} + \Delta S_{for} = 0$ ), the whole positive entropy contribution produced by folding is cancelled: the disruption of every hydrophobic bond is completed and the denatured state has become the stable one. The denaturation process, therefore, consists in the disruption, through cavity creation and negative entropy production of the entropy-driven hydrophobic bonds which had been keeping the chains folded.

The denaturation process can be represented also in a free-energy diagram (Fig.11). We refer

Fig. 11. a) Native folded state, stable ( $\Delta G_{fold}<0$ ) because entropy driven ( $\Delta S_{red}>>0$ )

b) Thermal denaturation at temperature  $T_d$ : after heat supply, melting of water  $W_{III}$  has created a cavity, entropy consuming.  $\Delta S_{for}<<0$  compensates for  $\Delta S_{red}>>0$ , leading to stable denatured state (unfolding) with  $\Delta G_{unfold}<0$ .

to the motive free energy of folding: a) (Fig.11,a) before heat supply starts, the folded native state is thermodynamically stable being, at any temperature, the motive (folding) free energy negative ( $\Delta G_{fold}<0$ ), due to the outstanding contribution of the positive entropy change ( $\Delta S_{red}>>0$ ), b) (Fig.11,b) after completion of heat supply, the folding free energy has become positive because the negative entropy change ( $\Delta S_{for}<<0$ ) due to cavity formation has completely cancelled the cavity reduction entropy gain at folding and hence the denaturation free energy is negative ( $\Delta G_{unfold}<0$ )

## 8. Chemical Denaturation and Template Effect

A proof of the constancy of slope  $\Delta C_p$ , and hence of  $\xi_w$ , in the denaturation enthalpy of proteins has been shown by Pfeil and Privalov [15]. They report a diagram where denaturation enthalpy of lysozyme conforms to Eq. (3) with a constant slope either when the denaturation is

Fig. 12. a) Lysozyme. The slope is constant (*i.e.*  $\Delta C_p$  is constant) whatever thermal or chemical denaturation and whatever the experimental method (Data from Privalov [16]).

obtained by thermal denaturation or by GuCl denaturation (Fig. 12). This means that also by changing the concentration of denaturant we obtain the same parallel displacement of curves as that shown by Lumry [12] by changing  $[H^+]$ . This behaviour suggests that the reaction mechanism could be the same in either situation. We can suppose, therefore, that in chemical denaturation we are dealing with at least two coupled equilibria, the first one is the dissociation from the bulk of water  $W_{III}$  with creation of the cavity, with equilibrium between the three forms of water ( $W_I$ ,  $W_{II}$ , and  $W_{III}$ ) and the second process is the binding of ligand, like a proton or a denaturant.

The type of binding between protein and ligand could be direct or mediated through water. In the thermal denaturation of chymotrypsinogen we succeeded to demonstrate the existence of a protonation constant  $K_{prot}$  coupled to the hydration reaction constant  $K_{hydr}$ .

S. N. Timasheff, *et al.* [21] have studied the role of solvation in protein stabilization and unfolding believing correctly that the problem of chemical denaturation is strictly connected to the opposite process of stabilisation. The types of denaturing and stabilising molecules are apparently different (Table 9). According to these authors, all denaturants examined (urea, guanidinium hydrochloride, 2-chloroethanol, methoxyethanol) should interact preferentially with proteins. Urea and guanidinium hydrochloride are supposed to interact with peptide groups, while the alcohols should interact with the non-polar residue, relieving the hydrophobic pressure of water and permitting the

structure to loosen. In regard to stabilisation, Timasheff *et. al.* observe that stabilizing agents are polyhydric compound containing solvents such as aqueous glycerol, sucrose, and hexylene glycol, (2-methyl-2,4-pentanediol (MPD)). Lee and Timasheff [22] have analysed the interactions with solvent components of proteins in guanidinium hydrochloride and propose an interaction between protein and denaturant mediated by an intimate contact between denaturants and portions of the protein molecule. Timasheff [23] finds, however, that the binding affinity of the chemical denaturants urea or GuHCl is rather low, similar to hydration affinity, and in fact the denaturant would be in competition with water for the same binding sites. In contrast, Poland [24], by examining the effect of GuHCl on the denaturation of ferro- and ferri-cytochrome C, concludes that free energy depends on changes of  $\log c$  ( $c = [\text{GuHCl}]$ ). He calculates two equilibrium constants,  $K(\text{II}) = 4.305 \cdot 10^{-8}$  for Fe(II) protein and  $K(\text{III}) = 1.079 \cdot 10^{-3}$  for Fe(III) protein. This means that GuHCl behaves, at least in this case, as a ligand forming a strong bond with the protein.

Fig. 13. The action of denaturant displaces the equilibrium in water toward formation of cavity with negative entropy production, that cancels the positive entropy gain of folding.

By considering that a direct protein-denaturant interaction might be responsible of the denaturing action we have analysed the data reported by Timasheff *et. al.*[21]. The analysis, however, has shown that in any case the affinity between protein and denaturant is very low and not sufficient to cancel the favourable entropy-driven affinity of folding. The interactions between protein and denaturant are not so strong to displace the denaturation equilibrium to the field where the denatured state is thermodynamically stable. J. A. Schellman [25] had arrived at the same conclusion that the interaction of urea with a protein site is extremely weak.

J. A. Schellman has analysed also the importance of the excluded volume effect in denaturation. He observes that in weak binding of denaturant to protein, the second virial coefficient is negative, thus showing a parallelism with cavity reduction of FCB model. In this contest it is worth noting that both the expansion of polypeptide chains in denaturants [26] (we

Table 9. Denaturants and stabilising molecules for proteins.

recall cavity formation in Class A of FCB model) and their contraction in stabilising osmolites [27] (we recall cavity reduction in Class B of FCB model) have been observed experimentally.

We can consider, at this point, that the direct binding, similar to that observed in protonation, might not always be necessary for denaturation. We can suppose that the action of the denaturant is analogous to that exerted by heat supply in thermal denaturation. The action of the denaturant (urea or guanidinium) on the equilibrium  $\mathbf{A}(-\xi_w W_I \rightarrow \xi_w W_{II} + \xi_w W_{III} + \text{cavity})$  is toward the formation of the cavity, by binding preferentially to molecules of water  $W_{II}$ , thus producing negative entropy for cavity formation. (Fig. 13). This negative entropy compensates for the positive entropy gain produced by folding and brings the protein toward the level where the denatured protein is stable. This behaviour of denaturant not dependent from direct urea/protein affinity, explains the denaturing action of other polar substances such as 2-Chloroethanol 40% or Methoxyethanol 40% that look suited to modulate, with their linear shape, the equilibrium between the various forms of water  $W_I$ ,  $W_{II}$ , and  $W_{III}$  toward  $W_{II}$  and cavity formation. We can speak of “*template effect*” on water structure. The stabilising agents, in contrast, should be structurally suited to modulate the equilibrium between the forms of water toward the preferential formation of water  $W_I$ , that presents

## 2-Chloroethanol



a tetrahedral structure, roughly speaking. This could explain in particular the stabilising action of TMAO [28]. By adding TMAO, the Bolen group was able to refold an altered form of ribonuclease that *per se* was unable to fold in a stable conformation. Another stabilizer is MPD, whose structure can be schematically represented by two tetrahedra joined by a common apex. K. Anand, D. Pal and R. Hilgenfeld [29] have analysed crystal structures of complexes formed by proteins with MPD.

### 2-methyl-2,4-pentanediol (MPD)

These authors suggest that MPD promotes stabilisation of the protein by preferential hydration, which is facilitated by attachment of MPD molecules to the hydrophobic surface. Translated into the terminology of FCB model this would mean a template effect for stabilisation of water  $W_I$  with cavity reduction.

The *template effect* of denaturants favouring water  $W_{II}$  and that of stabilisers favouring water  $W_I$  parallels the distinction between *chaotropic* substances (denaturants, structure breaking) and *kosmotropic* (stabilisers, structure making) [30, 31]. This dramatically biblical terminology looks rather out of place for a phenomenon that perhaps is only a question of a templating preference for water  $W_I$  rather than  $W_{II}$  or *vice versa*, with minimal differences in energy.

The weakness of the interaction between water and denaturant is in agreement with the action of various denaturants on folding/unfolding transitions. For example, when concentrated guanidinium hydrochloride is diluted out of a sample of chemically denatured hen lysozyme, the protein refolds, spontaneously. In other words, the folded state (cf. Fig. 11,a) is energetically favoured in the absence or scarcity of chemical denaturant. Therefore, when guanidinium concentration is low, the equilibrium between the different forms of water is no more displaced toward cavity formation and the protein goes back to the folded state.

## 9. Salting-out and salting-in

There is also correspondence between stabilizers and salting out substances like as ammonium sulphate,  $(NH_4)_2SO_4$ . This substance decreases the solubility of proteins and is

Fig. 14. Solubility of butane in aqueous solutions of urea and of guanidinium hydrochloride

employed to facilitate precipitation of the proteins. Ammonium sulphate gives origin in aqueous solution to two tetrahedral ammonium ions and one tetrahedral sulphate anion that are good templates for  $W_I$  and cavity reduction, similarly to the elements of Class B of FCB model. This behavior indicates definitely that the salting-out effect is a member of Class B in the realm of the hydrophobic hydration processes.

Fig. 15. Hydrogen bonding of water to urea (A) is less efficient than to guanidinium ion (B). Salting-in effect is lower in urea solutions than in guanidinium solutions.

On the other hand, there is correspondence between denaturants and salting-in substances, like potassium thiocyanate, KSCN, that increase the solubility of non-polar substances. Thiocyanate gives origin to a linear anion  $SCN^-$  that works as template for  $W_{II}$  and cavity formation, similarly to the elements of Class A of FCB model. Other very good templates for  $W_{II}$  and cavity formation are urea and GuHCl. A larger cavity facilitates acceptance of more solute molecules and hence an increase of the solubility. This behavior is indicative that salting-in effect is a hydrophobic hydration process belonging to Class A with cavity formation.

The salting-out effect is difficult to evaluate quantitatively but salting-in can be evaluated, by measuring the increase of solubility. Wetlaufer et al. [32] have studied the solubility of butane in urea solutions and in guanidium chloride solutions. Their results give us the chance to evaluate the validity of the hypothesis on the kind of templating action of these denaturants. On the basis of FCB model, the inspiring idea is that urea (or guanidinium) coupled to the reaction  $\mathbf{A}(-\xi_w W_I \rightarrow \xi_w W_{II} + \xi_w W_{III} + \text{cavity})$ , tends to associate to  $W_{II}$ , thus displacing the reaction toward the formation of the cavity. The solubilities of butane follow exponential curves: the curve for guanidinium hydrochloride is about three times steeper than that for urea (Fig.14). Actually, we can observe (Fig.15) that on the basis of the molecular structures, the possibilities of binding of water via hydrogen bonds  $\text{NH}\dots\text{O}$  to GuHCl (B) are more than those of urea (A). Therefore, guanidinium hydrochloride is about three times more efficient than urea in templating for solvent molecules  $W_{II}$  and cavity formation.

The solubilities of butane in urea and in GuHCl, reported as the function of  $\ln[\text{Denaturant}]$  give the following expressions:

$$\text{urea, } c_{butan} = -1.78 + 0.139 \ln [\text{urea}] \quad (R^2 = 0.9991)$$

$$\text{GuHCl, } c_{butan} = -2.54 + 0.398 \ln [\text{GuHCl}] \quad (R^2 = 0.9769).$$

At the moment, it is not clear the exact thermodynamic relationship connecting denaturant concentration to solubility of hydrocarbon. Probably, the thermodynamic relation depends on the type of reaction coupled to the reaction of cavity formation. It is evident, however, that the better efficiency of GuHCl rather than urea can be evaluated by the power of concentration,  $[\text{GuHCl}]^{0.398}$  with respect to  $[\text{urea}]^{0.139}$ , with a ratio  $0.398/0.139=2.864$  clearly dependent on the better ability of forming hydrogen bonds with  $W_{II}$ .

Other effect of salting-in can be found in the changes of denaturation free energy by addition of denaturant. According to Haynie [33], the action of denaturant on free energy is represented by

$$\Delta G_{den} = \Delta G_{den}^{\circ} - mc \quad (19)$$

where  $\Delta G_{den}^{\circ}$  is the free energy in the absence of denaturant,  $c$  is the denaturant concentration and  $m$  is a parameter that depends on temperature, pH, and, of course, the protein. In some cases, however, the dependence on denaturant concentration is decisively non linear.

These uncertainties in the type of dependence upon denaturation concentration, reflect the variety of possible reactions coupled to the reaction  $\mathbf{A}(-\xi_w W_I \rightarrow \xi_w W_{II} + \xi_w W_{III} + \text{cavity})$  of cavity formation.

## 10. Excess Urea

If the number  $\xi_w$  of molecules  $W_{III}$  is constant, the curvature of the plot  $\log Q_{den} = f(1/T)$  remains constant at the variation of denaturant concentration, similarly to the plots of Fig. 3. Creation of water  $W_{II}$  is accompanied by formation of a cavity, thus facilitating the insertion of the hydrocarbon chains of the denaturing protein in the solution. The constancy of  $\xi_w$ , however, is apparently not always maintained when the denaturation concentration is high enough, as shown by Pace and Tanford [34] for  $\beta$ -lactoglobuline. In fact, if we plot  $\log K_{den}$  vs.  $(1/T)$  for  $\beta$ -lactoglobuline at high concentration of urea, the curve begins to become smoother (Fig. 16). If we calculate the tangent to these curves at different temperatures and plot the tangents (*i.e.*  $\Delta H_{den}$ ) against the temperature  $T$ , we obtain values of  $\xi_w$  that are changing with the concentration of urea. The variation  $\Delta \xi_w$  is (Table 10) almost null from 4.42 M urea to 5.09 M urea ( $\xi_w$  changes from 118.2 to 117.7 with  $\Delta \xi_w = 0.5$ ), thus indicating that it is just at the end of constant  $\xi_w$  regime but becomes

Fig. 16.  $\beta$ -globuline: the curves are becoming smoother at high concentration of urea, i.e.  $\Delta C_p$  is sharply decreasing when urea concentration is large enough (From Ref. [34])

appreciable by passing from 5.09 M to 5.59 M ( $\xi_w$  changes from 117.7 to 92.1 with  $\Delta\xi_w = 25.6$ ). The slope of the line depends, according to FCB model, on the number  $\xi_w$  of water molecules  $W_{III}$ , experimentally determined by *TED*, set free to form a cavity to host the unfolded branches of the macromolecule. Because we do not think that a lower value of the number  $\xi_w$  could indicate a smaller cavity to host the same branches, we must conclude that the only explanation possible for the action of urea according to FCB model, is that urea itself promotes formation of  $W_{II}$  and melting of  $W_{III}$ . The molecules of denaturant in excess, however, at the higher concentrations begin to combine with the water molecules  $W_{III}$  set free by the reaction  $\mathbf{A}(-\xi_w W_I \rightarrow \xi_w W_{II} + \xi_w W_{III} + \text{cavity})$ .

Fig. 17. Solubility of hydrocarbons in water and urea at different temperatures.

Table 10. Denaturation of  $\beta$ -lactoglobuline. Change of number  $\xi_w$  at high urea concentration.

In such a way, the number  $\xi_w$  of free water  $W_{III}$  experimentally detected seems to correspond to a smaller cavity, what really is not the case. In fact, one part of the molecules  $W_{III}$  expelled from the cavity, has been sequestered by the excess of denaturant and is no more free and cannot be detected as such by *TED*

The binding of denaturant in excess to water  $W_{III}$  has been confirmed by analysing the solubility of hydrocarbons in water and in urea solutions at different temperatures as determined by Wetlaufer *et al* [32]. The curvatures of the solubility in water (Fig.17) are higher than those in concentrated urea. This shows that in urea solutions the number  $\xi_w$  is smaller than in water (Table 11), because in these cases again one fraction of water  $W_{III}$  expelled from the cavity is absorbed by

Table 11. Curvatures ( $\xi_w$ ) of hydrocarbons solubility in water, and in concentrated urea solution.

urea in excess and cannot be detected as free by mean of *TED*.

## 11. Comparisons with Molecular Calculations

The conclusions of FCB model can be compared with the results of molecular calculations that have been applied in many cases to the hydrophobic processes.

F. Vanzi, B. Madan, K.Sharp [35] have analysed the effect of the protein denaturants urea and guanidinium on the water structure. Changes in the hydrogen bonds network of water in the first hydration shell were analysed in terms of the random network model (RNM) using Monte Carlo simulations. According to their results, bulk water consists of two populations of hydrogen bonds: a predominantly linear population and a small but significant population of slightly longer and more bent hydrogen bonds. In a previous work [36] K.A. Sharp and B. Madam had shown that it is possible to distinguish two hydrogen bond populations: a larger population with quasi tetrahedral ice-like population with  $\theta_h \approx 12^\circ$  and a smaller population in which a fifth molecule, a mismatch water comes into the coordination shell of the central water molecule, forming a highly distorted H-bond with  $\theta_h \approx 52^\circ$ . We can identify the former population with water  $W_{II}$  and the

latter population with water  $W_I$ . They have also found that non polar solutes (comparable to Class A of FCB model) tend to decrease the second population by competing for the position of the mismatch water molecule. Polar solutes, however, have the opposite effect, comparable to Class B of FCB model. They recall two of the possible binding mechanisms put forward by Wetlaufer *et al.* [32]: one mechanism postulated for the denaturing activity of urea and guanidinium involves binding to protein groups exposed to solvent. Another possible mechanism is through effect on water structure, and thus on the strength of the hydrophobic effect. They state, however, that demonstrating that this mechanism, rather than direct binding to protein groups, is sufficient to denature proteins has proved to be elusive. A necessary condition for the direct effect on water structure should be, according to Sharp and Madam, that these denaturants affect the structural and thermodynamic properties of water in a unique way (unique in the sense that distinguishes them from the effect on water of solutes that are *nondenaturing*).

Particularly they underline the fact that the hydrogen bond angle between waters in the first hydration shell, is a powerful way to analyse solute-induced perturbations for two reasons: (1) It is sensitive to structural perturbations, (2) The structural changes may be directly and quantitatively related to a key thermodynamic property, the heat capacity  $\Delta C_p$ . Ample experimental data (we can recall our Eq. (1) and comments thereafter) have shown that hydration heat capacity change is the most revealing of the common thermodynamic functions (the others being free energy, enthalpy, and entropy) in terms of the differences between hydration of polar and non-polar (hydrophobic) solutes.

From this point on, however, the correspondence with FCB model is failing. In fact, according to our calculations, heat capacity ( $\Delta C_p = \xi_w C_{p,w}$ ) is bound to the reaction of water  $W_{III}$  whose stoichiometric coefficient  $\xi_w$  has been determined by us making use of *TED*. In the absence of the essential component  $W_{III}$ , the model of Sharp and Madam cannot explain the formation of cavity and the related relevant entropy change. The origin also of thermal enthalpy,  $\Delta H_{therm}$  and thermal entropy,  $\Delta S_{therm}$  and their strict interrelationship ( $\Delta S_{therm} = \Delta H_{therm}/T$ ) cannot be explained, and many other properties of the systems, as well.

According to the calculations of Widom, Bhimalapuram, and Koga [37], the hydrophobic effect both as cause of low solubility or of hydrophobic bonding, can be satisfactorily explained by referring to a Ising lattice model in Bethe-Guggenheim approximation. Alternatively the same approximation they obtain by Montecarlo calculations. Both methods reach the conclusion that hydrophobicity is temperature dependent, in agreement with the conviction that the hydrophobicity effect becomes stronger with increasing temperature. These conclusions are clearly in contrast with our findings that the effect of the temperature on hydrophobic solubility and hydrophobic bond is due exclusively to the transformation undergone by water  $W_{III}$  ( $\Delta S_{therm}$  and  $\Delta H_{therm}$ ). The actual hydrophobic repulsion (Class A) is independent from the temperature and is ruled by the negative entropy change ( $\Delta S_{for} \ll 0$ ) associated to cavity formation. The hydrophobic attraction or hydrophobic bond (Class B) is again independent from the temperature and ruled by the positive entropy change ( $\Delta S_{red} \gg 0$ ) associated to cavity reduction. Therefore also the model of Widom, Bhimalapuram, and Kohas has to be considered as inadequate to explain the hydrophobic effects.

P. J. Rossky [38] thinks that some of the earlier discussions on the mechanism of unfolding by urea focused on perturbation of water structure per se (Frank and Franks [6]), the so-called “indirect” mechanism has not received much support from experimental or simulation studies of aqueous urea. The alternative “direct” mechanism, implying a causative interaction between urea and the polypeptide, has been clearly evidenced, according to P. J. Rossky, in the simulated pathways. This point of view of Rossky is clearly in contrast with the conclusions of our work.

These are not the only discrepancies between FCB model and the theoretical models proposed in the literature. In fact, a surprising feature of the unitary thermodynamic functions calculated by us for the various steps of all the hydrophobic processes ( $\langle \Delta h_{for} \rangle_A = -22.2 \pm 0.7$  kJ·mol<sup>-1</sup>· $\xi_w^{-1}$ , and  $\langle \Delta s_{for} \rangle_A = -445 \pm 3$  J·K<sup>-1</sup>·mol<sup>-1</sup>· $\xi_w^{-1}$  in Class A, and  $\langle \Delta h_{red} \rangle_B = +23.7 \pm 0.6$  kJ·mol<sup>-1</sup>· $\xi_w^{-1}$ , and  $\langle \Delta s_{red} \rangle_B = +432 \pm 4$  J·K<sup>-1</sup>·mol<sup>-1</sup>· $\xi_w^{-1}$  in Class B) is that they have been calculated by

including results obtained from both large and small molecules. This indicates that the same type of unitary reaction is taking place in every case, independently from the total size of the reactant. This result is very important because it is in contrast with some theories supported by molecular calculations[39, 40]. According to Chandler [39], there should be a cross-over point of behaviour by the solvent, passing from small to large solutes. The solute of small size should accommodate within the interstices of the structure of water, whereas, beyond a certain length-scale of the molecule, a type of molecular hydrophobic interface in the solvent should become thermodynamically and energetically feasible. In the former case the hydrophobic effect would be proportional to the volume of the small solute, whereas in the latter the effect would be proportional to the surface of the large solute molecule. The passage from one another type of reaction would take place at a specific cross-over point that can be calculated by an appropriate algorithm. Actually, according to FCB model, the type of reaction in the solvent is the same both in small and large molecules: it is the transformation  $\mathbf{A}(-\xi_w \mathbf{W}_I \rightarrow \xi_w \mathbf{W}_{II} + \xi_w \mathbf{W}_{III} + \text{cavity})$ .

The point of view of Chandler is reinforced by S. Rajamani, *et al.* [40] who write that as the solute size is increased, water dewets the solute surface. Near a sufficiently large solute, the solute-solvent interface should resemble that between vapour and liquid water, and therefore should require interfacial thermodynamics for its recognition. Correspondingly, the thermodynamics of hydration should change gradually from entropic for small solutes to enthalpic for large solutes. The theoretical approach by Lum *et al.*[41] provided a quantitative description of structural and thermodynamic aspects of hydrophobic hydration over the entire small-to-large length scale region.

Fig. 18. a) Small molecule: the cavity surrounds the whole molecule; the trapped gas molecules lose their configurational entropy ( $\Delta S_0^{(\xi_w=0)} = -86.4 \text{ J}\cdot\text{K}^{-1}\cdot\text{mol}^{-1}$ )

b) Macromolecule: the cavity surrounds only the unfolded chains; the core C remains almost invariant but the solvent volume is reduced and the solute becomes more concentrated ( $\Delta S_0^{(\xi_w=0)} = -59.7 \text{ J}\cdot\text{K}^{-1}\cdot\text{mol}^{-1}$ ).

Yamirsky and Vogler [42] share this point of view that there is a gradual passage from small to large scale because they organize their article around length scale as a means of resolving commonalities between seemingly disparate phenomena that are all outcomes of hydrophobic hydration. Their major section is concerned with hydrophobic (dissolution) of small hydrophobic molecules such as methane and extends this discussion to self assembly or aggregation of hydrophobic molecules in a manner consistent with what has become a traditional bifurcation of hydrophobic effects into two categories: (i) hydrophobic hydration, (ii) hydrophobic bonding. These authors, however, are sceptical about the possibility that theoretical simulations of the behaviour of too few molecules near hydrophobic interloper are suitable to reveal an alteration in vicinal water density brought about by a collective change in self association. At the same time, they are dubious about the capacity of a thermo-chemical experiment involving too many water molecules to reveal the averaging behaviour of the relatively few water molecules in direct contact with hydrophobic entity. After such uncertain statements, there is little wonder how the hydrophobic hydration literature has become so entangled.

The contradictions of these statements with the conclusions of FCB model are apparent. The antinomy large/small scale, however, is resolved if we keep that the denaturation is characterized by the creation of a cavity in the solvent to allocate only the unfolded chains of the macromolecule, in the same way as this occurs, for the entire molecule, with small compounds (Fig.18). It is sufficient to admit that in large molecules, the number of unfolding chains is proportional to the surface of the macromolecule, what is reasonable, and the contradiction disappears.

We should reject, however, the idea that a certain type of molecular hydrophobic interface in the solvent, typical of large scale molecules might become thermodynamically and energetically

feasible. This misunderstanding on the structure of the solvent has been probably born by the fact that a change of mechanism exists on the side of the solute. In fact, with small molecules, we are dealing with a solubilisation process from gas to solution whereby the whole molecule needs a cavity large enough to surround the whole molecule. According to the FCB model, the solubility reaction, that belongs to Class A, can be subdivided in successive steps. The first step consists in the passage of the molecules from the disordered gaseous state to the condensed state trapped in the cavity of the solvent. Associated to this step<sup>4</sup>, there is an extrapolated (cf. Eq.12) entropy change  $\Delta S_0^{(\xi_w=0)} = -86.4 \text{ J}\cdot\text{K}^{-1}\cdot\text{mol}^{-1}$ , that measures the loss of configurational entropy by the trapped molecules. It is worth noting that in the solubility of liquids the same step entropy<sup>5</sup> is practically null ( $\Delta S_0^{(\xi_w=0)} = -0.5 \text{ J}\cdot\text{K}^{-1}\cdot\text{mol}^{-1}$ ). The lack of entropy loss in the liquids is in accordance with the absence of translational entropy. In fact, the liquids, before being dissolved, are already condensed. For macromolecules we can consider as process of Class A the denaturation reaction. The process of unfolding involves only the hydrophobic chains of the external surface. Each chain needs a cavity proportional to its own volume only, to be allocated. The core of the macromolecule, instead, constitutes a volume excluded to the solvent both before and after unfolding. In regard to the process of folding/unfolding the core volume undergoes minor changes. The corresponding negative step entropy in the group of proteins examined is  $\Delta S_0^{(\xi_w=0)} = -59.7 \text{ J}\cdot\text{K}^{-1}\cdot\text{mol}^{-1}$  (cf. Table 3) and is probably due to an increase of the concentration of the solute caused by the sum of the cavities allocating the unfolded chains. The sum of cavities represents, in fact, further volume excluded to the solvent.

All these notes about the specificities of the extrapolated entropy in different families of reactions of Class A demonstrate unequivocally that it is in the properties of the solute that we can find discontinuities or cross-over points, but not in the behaviour of the solvent. It is clear that on the side of the solvent, the only and the same type of reaction  $\mathbf{A}(-\xi_w W_I \rightarrow \xi_w W_{II} + \xi_w W_{III} + \text{cavity})$  has taken place, both in small and large molecules.

The problem of the bifurcation of hydrophobic effects into two categories is brilliantly resolved in FCB model by the subdivision of the hydrophobic hydration processes into the two classes A and B, with their types of reactions, direct or inverse, respectively. At the same time, the effect of few molecules  $\xi_w W_{III}$  contributing exclusively to both thermal enthalpy and thermal entropy is suitable to reveal, by thermodynamic experiments based on *TED*, the changes with temperature of the thermodynamic functions. These few water molecules  $W_{III}$ , in thermal denaturation, become, through their passage of state from structure to fluid or vice versa, the key to open the zip fastener formed by the entropy-driven hydrophobic bonds that had been keeping the chains folded in the native state.

Other authors, however, have put forwards ideas conforming more or less with FCB model. H. S. Frank and M. W. Evans [43] and G. Nemethy and H. A. Scheraga [44] suggested that water is caging around non-polar gases, a distorted structure enabling the maintenance of hydrogen bonds that water cannot form with the hydrophobic core. In the process of this rearrangement, enthalpy is gained (cf.  $\Delta H_{for} = -\xi_w \cdot 22.5 \text{ kJ}\cdot\text{mol}^{-1}$ , with unitary enthalpy change  $\Delta h_{for} = -22.5 \text{ kJ}\cdot\text{mol}^{-1} \cdot \xi_w^{-1}$ ) at the expense of entropy loss (cf.  $\Delta S_{for} = -424.2 \xi_w \text{ J}\cdot\text{K}^{-1}\cdot\text{mol}^{-1}$ , with unitary entropy change  $\Delta s_{for} = -424.2 \text{ J}\cdot\text{K}^{-1}\cdot\text{mol}^{-1} \cdot \xi_w^{-1}$ ). The point concerning entropy loss for cavity formation is accepted by Graziano [45] who asserts, however, that insertion of a solute molecule in a liquid phase significantly restricts the configurational space accessible to solvent molecules, providing a large and negative entropy change. This assertion by Graziano is in contrast with the FCB model, that considers that the configuration entropy loss  $\Delta S_{for} \ll 0$  is referred to the solute that is now more concentrated in a smaller volume, whereas  $\xi_w$  water molecules  $W_{III}$  expelled from the solvent to form the cavity (*i.e.* the excluded volume effect) acquire the thermal entropy  $\Delta S_{therm} = \xi_w C_{pw} \cdot \ln T > 0$ .

<sup>4</sup> cf. Ref. [4], paragr. 6.1, p. 124

<sup>5</sup> cf. Ref. [4], paragr. 6.2, p. 126

H. Frank and F. Franks [6] have proposed a mechanism of unfolding focused on perturbation of water structure by urea, a mechanism that is similar to that proposed by us in the present model. Y. D. Livney, R. Edelman, I. Kusner, R. Kisiliak, S. Srebnik [46] have combined mathematical modelling and laboratory experiments to study the stereochemical structure effect on hydration of three isomeric aldohexoses: glucose, galactose, and mannose. The atomistic simulation was developed and used to quantify the compatibility of each aldohexose molecule with ideal tetrahedral water structure as embodied in hexagonal ice. These results support the template concept, proposed by FCB model, as the basis to explain the stabilizing effect of these substances on the water structure  $W_I$ .

## 12. Conclusions

The analysis of free energies, enthalpies, entropies of protein denaturation has shown that the model proposed for the hydrophobic hydration processes is suitable to explain the thermodynamic changes occurring in protein denaturation. Application of *TED* principle has made possible the determination of the number  $\xi_w$  of water molecules  $W_{III}$  involved in each denaturation process. The  $\xi_w$  water molecules  $W_{III}$ , ( $\xi_w > 0$ ) released in the denaturation process correspond to the formation of a cavity to host the unfolding branches of the macromolecule. The molecular mechanism of cavity formation in the solvent structure is the same as that in inert gas solubilisation. The change of phase of  $\xi_w$  water molecules  $W_{III}$ , expelled to form the cavity, is the only reaction that generates the high value of the isobaric heat capacity  $\Delta C_p$  at denaturation and consequently these water molecules are the only contributors to the thermal enthalpy,  $\Delta H_{therm} = T\Delta C_p$  and to the thermal entropy,  $\Delta S_{therm} = \ln T \Delta C_p$ . The decisive role of these water molecules with their change of phase in the denaturation process have to be stressed upon. Coupled to this process of melting, other processes of cavity formation and of protonation are active at denaturation. This demonstrates that, notwithstanding the doubts raised by Winzor and Jackson [11], it is possible to arrive at a complete thermodynamic description of protein interactions.

We can recall that in the folding of proteins, in contrast to denaturation, the number  $-\xi_w$  of water molecules  $W_{III}$  corresponds to a process of cavity reduction with production of positive entropy and formation of hydrophobic bonds, the same process that takes place in micelle formation. The thermal denaturation consists, therefore, in the gradual disruption by the heat supplied, via the production of negative entropy for cavity formation, of the entropy-driven hydrophobic bonds that had been keeping the chains folded. The action of chemical denaturants like as urea, guanidinium chloride or others is similar to that exerted by heat. The denaturant displaces the equilibrium  $\mathbf{A}(-\xi_w W_I \rightarrow \xi_w W_{II} + \xi_w W_{III} + \text{cavity})$  toward the formation of the cavity, with production of negative entropy. By considering that the stabilizing substances affect this equilibrium in the opposite way favouring the formation of water  $W_I$ , this proves that these denaturants affect the structural and thermodynamic properties of water in a unique way (unique in the sense that distinguishes them from the effect on water of solutes that are *nondenaturing*), as required by Sharp and Madam [36]. The comparison of the specific characteristics of the present model with the result of the many molecular calculations has revealed that some points of agreement exist, mainly in the simulations of Sharp and Madam [36]. Two decisive features, however, are in contrast with FCB model: (i) the separation between thermal and motive components of the thermodynamic functions is not taken into account in the molecular calculations, thus ignoring the specific behaviour of water  $W_{III}$ , associated to the thermal components, as well as the process of cavity formation, associated to the motive components; (ii) the cross-over point described by the molecular calculations for the behaviour of the solvent when passing from small to large molecules of solute is absolutely excluded by FCB model.

The separate enthalpy and entropy terms attributable to the different steps of the hydrophobic hydration processes are numerically very close to each other, respectively, in the different processes and the results of the present research on denaturation confirm those findings.

### Appendix A.

#### Denaturation Equilibria and Thermodynamic Functions

The equilibrium between native  $N$  and denatured  $D$  state of a protein can be decomposed into two steps. The first process is the conformational transition from the  $D$  to  $N$  state with the constant  $Q_{conf}$

$$Q_{conf} = [D]/[N] \quad (\text{A.1})$$

The second process is the hydration of the denatured state via the formation of a cavity in the bulk of the solvent molecules by expulsion of water molecules  $W_{III}$



with equilibrium constant

$$K_{hydr} = [D_w] \cdot [(W_{III})_T]^{\xi_w} / [D] \quad (\text{A.3})$$

where  $[D_w] \gg [D]$  is the concentration of hydrated denatured molecules,  $[(W_{III})_T]$  is the activity<sup>6</sup>, temperature dependent, of water molecules  $W_{III}$ , and  $\xi_w$  is the number of water molecules expelled from the bulk to form a cavity. By substitution of eq (A.1) into Eq. (A.3) we obtain

$$K_{hydr} Q_{conf} = [D_w] \cdot [(W_{III})_T]^{\xi_w} / [N] = K_0 \quad (\text{A.4})$$

The denaturation quotient is (cf. Eq. (B.4))

$$Q_{den} = [D_w] / [N] \quad (\text{A.5})$$

and then by introducing Eq. (A.3) and Eq. (A.4) into Eq. (A.5), we obtain

$$Q_{den} = K_0 \cdot [(W_{III})_T]^{\xi_w} \quad (\text{A.6})$$

By taking the logarithms and multiplying by  $R$ , we obtain

$$R \ln Q_{den} = R \ln K_0 - \xi_w R \ln [(W_{III})_T] \quad (\text{A.7})$$

By differentiation with respect to  $(1/T)$ , we obtain

$$R \partial \ln Q_{den} / \partial (1/T) = R \partial \ln K_0 / \partial (1/T) - \xi_w R \partial \ln [(W_{III})_T] / \partial (1/T) \quad (\text{A.8})$$

By applying the van't Hoff Eq. (1) to Eq. (A.8), the denaturation enthalpy  $\Delta H_{den}$  is obtained as

$$\Delta H_{den} = \Delta H_0 + \xi_w R \partial \ln [(W_{III})_T] / \partial (1/T) \quad (\text{A.9})$$

<sup>6</sup> For a definition of activity and thermal equivalent dilution see Ref. (4), Appendix B



The last term of this equation can be rearranged as derivative with respect to  $\ln T$

$$+ \xi_w R \partial \ln[(W_{III})_T] / \partial (1/T) = - \xi_w RT \partial \ln[(W_{III})_T] / \partial (\ln T) \quad (\text{A.10})$$

and then by recalling the principle of equivalent thermal dilution (*TED*) [4]

$$- \xi_w R \partial \ln[(W_{III})_T] / \partial (\ln T) = \xi_w C_{p,w} \quad (\text{A.11})$$

where  $C_{p,w}$  is the isobaric heat capacity of water, we obtain

$$\Delta H_{den} = \Delta H_0 + \Delta C_p T = \Delta H_0 + \xi_w T C_{p,w} \quad (\text{A.12})$$

This means that if we plot the denaturation enthalpy against  $T$ , we should obtain a straight line with slope  $\Delta C_p = \xi_w C_{p,w}$ .

The passage from  $\ln Q_{den}$  via Eq. (A.8) to  $\Delta C_p$  of Eq. (A.12) takes place through a double derivation. In fact, the first derivative of Eq. (1) (van't Hoff equation) can be rearranged as

$$\begin{aligned} -\partial(R \ln Q_{den}) / \partial (1/T) &= -\partial(-\Delta G_{den}/T) / \partial (1/T) \\ &= -\partial(\Delta G_{den}) / (\partial \ln T) = \Delta H_{den} \end{aligned} \quad (\text{A.13})$$

then the second derivative can be calculated as

$$\partial(\Delta H_{den}) / \partial T = -\partial^2(\Delta G_{den}) / (\partial \ln T \partial T) = \Delta C_p \quad (\text{A.14})$$

At the same time, however, we can calculate the entropy change  $\Delta S_{den}$  as the first derivative of  $-\Delta G_{den}$  as

$$\partial(-\Delta G_{den}) / \partial T = \Delta S_{den} \quad (\text{A.15})$$

and then by recalling  $dS = C_p d \ln T$ , the second derivative can be calculated as

$$\partial(\Delta S_{den}) / \partial \ln T = -\partial^2(\Delta G_{den}) / (\partial T \partial \ln T) = \Delta C_p \quad (\text{A.16})$$

The equality of Eq. (A.14) and Eq. (A.16) means that if we plot  $\Delta S_{app}$  against  $\ln T$  we should obtain the same slope  $\Delta C_p$  as from the function  $\Delta H_{app} = f(T)$  and, therefore, we should obtain the same value of  $\xi_w$ , as already obtained in the solubilisation of inert gases ( $\xi_w > 0$ ) or in micelle formation ( $\xi_w < 0$ ).

## Appendix. B.

### Denaturation Free Energy and pH

We have tried to look deeper into the problem of the determination of free energy at different pH levels and different temperatures. The equilibrium constants calculated from the actual values of free energy  $\Delta G_{den}$  reported by Lumry et al. [12] are not exactly equilibrium constants, rather they are concentration quotients that are related to the equilibrium constants, with properties similar to those of the equilibrium constants. In fact, we can assume that the denaturation process is ruled by

an equilibrium between denatured protein, native protein and proton. If we indicate by  $[D_w]$  the concentration of the hydrated denatured protein, by  $[NH_x]$  the concentration of the protonated native protein, and by  $[H^+]$  the concentration of proton, the equilibrium can be written



with equilibrium constant

$$K_{den} = [D_w] \cdot [NH_x]^{-1} \cdot [H^+]^x \quad (B.2)$$

which includes the constant  $K_{hydr}$  of Eq. (A.4). By considering that the protein concentration is  $[P]$  and that  $[NH_x]/[P] = \alpha$  and  $[D_w]/[P] = (1-\alpha)$  this expression can be rewritten as

$$K_{den} = ((1-\alpha) / \alpha) [H^+]^x \quad (B.3)$$

and by introducing the denaturation quotient

Fig. B.1. Determination of denaturation free energy at different pH and different temperatures. The curve at each pH is the branch  $br_j$  (pH=3, or 2.4,...) with origin at  $O_j$ .

$$Q_{den} = (1-\alpha) / \alpha \quad (B.4)$$

and rearranging, we obtain

$$[H^+]^{-x} K_{den} = Q_{den} \quad (B.5)$$

where  $Q_{den}$  is the quotient determined by Lumry [13] as free energy  $\Delta G_{den} = -2.302 RT \log Q_{den}$ . The values of free energy reported at different temperatures for each value of pH are those around  $Q_{den} = 1$ .

The equation (B.5) shows how the ratio  $Q_{den}$  has important properties in common with the dissociation constant  $K_{den}$ . By taking the logarithm (we use the decimal logarithm in order to be on the same scale as pH) we obtain

$$\log[H^+]^{-x} + \log K'_{den} = \log Q_{den} \quad (B.6)$$

where  $K'$  is a conditional dissociation constant, holding at  $pH = 2$

We can show that the derivatives of both members of Eq. (B.6) with respect to temperature and pH are the same, namely

$$\partial(\log[H^+]^{-x})/\partial pH = \partial \log Q_{den} / \partial pH \quad (B.7)$$

and (van't Hoff)

$$\partial \log K'_{den} / \partial (1/T) = \partial \log Q_{den} / \partial (1/T) \quad (B.8)$$

This derivative has been calculated in Eq. (A.8) and Eq. (A.9). The equality of Eq. (B.8) is also valid for the integrals

$$\int_{T_1}^{T_2} \partial \log K'_{den} / \partial (1/T) d(1/T) = \int_{T_1}^{T_2} \partial \log Q_{den} / \partial (1/T) d(1/T) \quad (B.9)$$

$$T_1 \qquad T_1$$

What means that the trend of the curve representative of  $\log K_{den}$  as the function of  $(1/T)$  is the same as that of  $\log Q_{den} = f(1/T)$ , *i.e.* it is a curve with a minimum.

By choosing a pH such that

$$\log[H^+]^{-x} + \log K'_{den} = 0 \quad (B.10)$$

we have  $\log Q_{den} = 0$ . Now, we can determine several values of  $\log Q_{den}$ , for example at pH =2 (Fig. 5), around the origin  $O_1$ , by changing the temperature. We thus obtain the branch  $br_{1(pH=2)}$  of the curve  $\log Q_{den} = f(1/T)$ . If we change pH again, we introduce a change  $\Delta(\log[H^+]^{-x})$ : then we can find

$$-\Delta(\log[H^+]^{-x}) = (1/2.302) \int_{T_1}^{T_2} \partial \log K'_{den} / \partial (1/T) d(1/T) \quad (B.11)$$

Fig. B 2. Sections of the cumulative denaturation curve can be moved to the range of  $\log Q$  around 0 by increasing pH. The shape of the curve is invariant because  $\Delta C_p$  is constant.

a new value of  $\log K'_{den}$  satisfying the condition of Eq. (B.10), if we change the temperature in such a way that  $\log K_{den}$  changes by an amount exactly opposite to the variation of  $\Delta(\log[H^+]^{-x})$  with pH. We now determine some values of  $\log Q_{den}$  around the new origin  $O_2$  (*i.e.* around  $\log Q_{den} = 0$ ) by

Fig. B.3. The cumulative curve obtained by displacement of each branch to pH = 0. At the right hand, the scale for displacement to pH =2: the curve is partially in the negative field of  $\log Q_{den}$

changing the temperature around  $1/T_2$  of  $O_2$ . We thus construct the new branch  $br_{2(pH=2.15)}$  around the middle point  $O_2$  (at  $\log Q_{den} = 0$ ) analogous to  $br_{1(pH=2)}$ . The trend of  $br_{2(pH=2.15)}$ , however, is different from the trend of  $br_{1(pH=2)}$ , because it is equal to that of  $\log K_{den}$  (and then of  $\log Q_{den}$ ) in a different range of higher temperatures. If we know in some way or can determine the amount of the change  $\Delta(\log[H^+]^{-x})$ , we can displace upward the origin of  $br_{2(pH=2.15)}$  and all of its experimental points, parallel to the ordinate axis, by an amount equal to  $-\Delta(\log[H^+]^{-x})$ . This parallel displacement can be found graphically in such a way to insert  $br_{2(pH=2.15)}$  just in continuity or in partial overlapping with the previous  $br_{1(pH=2)}$ . By repeating this procedure at other values of pH, we can construct the whole curve for a large interval of temperatures. Obviously, the displacement of  $br_{1(pH=1.6)}$  is downward. A schematic diagram showing the decomposition/composition procedure of the denaturation curve is shown in Fig. B2. The cumulative function with all the curves displaced to pH=2 is reported in Fig. B.3. If the cumulative curve is further displaced to pH=0 the whole curve fall in the range of positive  $\log K$ , thus indicating the reaction has been brought to the range where denaturation is thermodynamically favoured.

If we plot the values graphically determined of  $-\Delta(\log[H^+]^{-x})$  versus  $\Delta(\text{pH})$ , *i.e.* the variation with respect to pH=2, we obtain the equations reported in Table B.1. From the slope of these equations, we calculate the power  $x$ , that is related to the number of protonated sites on the protein. This power results to be  $\langle x \rangle = 3.04 \pm 0.08$  and hence the integer 3 for every compound examined. The higher is the hydrogen ion concentration added ( $\Delta(\text{pH}) < 0$ ), the larger is the displacement

Table B.1. Relationships between  $\Delta(\log[H^+]^{-x})$  and  $\Delta(\text{pH})$   
 $\langle x \rangle = 3.04 \pm 0.08$

upward applied to the equilibrium constant in the diagram. That means that the association between denatured protein and proton is increased by the addition of hydrogen ions. Alternatively to the graphical method, we can calculate mathematically the displacements of the branches, according to the following procedure. Calculate the interpolation polynomial of  $br_{1(pH=2)}$  thus obtaining the function  $F_1$  with origin  $O_1$  and the interpolation polynomial of  $br_{2(pH=2.15)}$ , thus obtaining the function  $F_2$  with origin  $O_2$ . Calculate the abscissa  $1/T_1$  of  $O_1$  and calculate the value of  $F_1$  at this temperature  $T_1$ . This value of the function  $F_1$  corresponds to the increment to assign to each experimental point of  $br_{2(pH=2.15)}$  to bring them on the same curve of  $br_{1(pH=2)}$ . We compose a new cumulative branch  $br_{1,2(2+2.15)}$  interpolated by a new function  $F_{(1,2)}$  with origin at  $O_1$ . Then we pass to  $br_{3(pH=2.4)}$  and calculate the interpolation polynomial  $F_3$  with origin at  $O_3$ . We calculate the abscissa  $1/T_3$  of  $O_3$  and then calculate the value of the function  $F_{(1,2)}$  at this point. This value is the displacement applied to all the experimental points of  $br_{3(pH=2.4)}$  in order to bring them on the same curve of  $br_{1,2(2+2.15)}$ . We compose a new cumulative  $br_{1,2,3(2+2.15+2.4)}$  for which we can calculate the interpolation function  $F_{(1,2,3)}$  with the old origin  $O_1$ . We continue these steps till the last branch is included in the total set. Obviously, the displacement of  $br_{-1(pH=1.6)}$  with origin at  $O_{-1}$  is negative.

## Acknowledgements

This work was supported by the contributions from the Cassa di Risparmio di Parma Foundation and the University of Parma.

Professor G.P. Chiusoli, Emeritus, University of Parma, is warmly thanked for assistance in the presentation of the paper.

## Glossary

- Class A = Processes with transformation  $\mathbf{A}(-\xi_w W_I \rightarrow \xi_w W_{II} + \xi_w W_{III} + \text{cavity})$   
 Class B = Processes with transformation  $\mathbf{B}(-\xi_w W_{III} - \xi_w W_{II} \rightarrow \xi_w W_I - \text{cavity})$   
 $W_I$  = water cluster  $(W_5)_I$ ,  
 $W_{II}$  = water cluster  $(W_4)_{II}$   
 $W_{III}$  = free water molecule  
 $\pm \Delta W_I$  = water  $W_I$  changing to form or reduce cavity  
 $+\xi_w$  = number of water molecules  $W_{III}$  expelled from cavity  
 $-\xi_w$  = number of water molecules  $W_{III}$  restructured to reduce cavity  
*TED* = *thermal equivalent dilution* (Ergodic Hypothesis)  
 FCB = Fisicaro, Compari, Braibanti  
 $\Delta H_{app}$  = apparent enthalpy (experimental enthalpy in a general hydrophobic process)  
 $\Delta H_{den}$  = denaturation enthalpy ( $\equiv \Delta H_{app}$ )  
 $\Delta H_{(0)}$  =  $\Delta H_{den}$  extrapolated to  $T=0$   
 $\Delta H_{mot}$  = motive component of enthalpy ( $\equiv \Delta H_{(0)}$ )  
 $\Delta H_{den}$  =  $\Delta H_{mot} + \Delta H_{therm}$   
 $\Delta H_{therm}$  = thermal component of enthalpy ( $= +\Delta C_p T$  in Class A)  
 $\Delta H_{mot}$  =  $\Delta H_0^{(\xi_w=0)} + \Delta H_{for}$   
 $\Delta H_0^{(\xi_w=0)}$  =  $\Delta H_{mot}$  extrapolated to  $\xi_w=0$  (no cavity,  $\Delta H_{for}=0$ )  
 $\Delta H_{for}<0$  =  $\xi_w \cdot \Delta h_{for}$  enthalpy change for cavity formation

- $\Delta h_{for}$  =  $-22.5 \text{ kJ}\cdot\text{mol}^{-1}\cdot\xi_w^{-1}$ , unitary enthalpy change for cavity formation  
 $\Delta H_{red}>0$  =  $\xi_w \cdot \Delta h_{red}$  enthalpy change for cavity reduction  
 $\Delta h_{red}$  =  $+22.5 \text{ kJ}\cdot\text{mol}^{-1}\cdot\xi_w^{-1}$ , unitary enthalpy change for cavity reduction  
 $\Delta S_{app}$  = apparent entropy (experimental entropy in a general hydrophobic process)  
 $\Delta S_{den}$  = denaturation entropy ( $\equiv \Delta S_{app}$ )  
 $\Delta S_{(0)}$  =  $\Delta S_{den}$  extrapolated to  $\ln T=0$   
 $\Delta S_{mot}$  = motive component of entropy ( $\equiv \Delta S_{(0)}$ )  
 $\Delta S_{den}$  =  $\Delta S_{therm} + \Delta S_{mot}$   
 $\Delta S_{therm}$  = thermal component of entropy (=  $+\Delta C_p \ln T$  in Class A)  
 $\Delta S_{mot}$  =  $\Delta S_0^{(\xi_w=0)} + \Delta S_{for}$   
 $\Delta S_0^{(\xi_w=0)}$  =  $\Delta S_{mot}$  extrapolated to  $\xi_w = 0$  (no cavity,  $\Delta S_{for} = 0$ )  
 $\Delta S_{for}<0$  =  $\xi_w \cdot \Delta s_{for}$ , entropy change for cavity formation  
 $\Delta s_{for}$  =  $-445 \pm 3 \text{ J}\cdot\text{K}^{-1}\cdot\text{mol}^{-1}\cdot\xi_w^{-1}$ , unitary entropy change for cavity formation  
 $\Delta S_{red}>0$  =  $\xi_w \cdot \Delta s_{red}$ , entropy change for cavity reduction  
 $\Delta s_{red}$  =  $+432 \pm 4 \text{ J}\cdot\text{K}^{-1}\cdot\text{mol}^{-1}\cdot\xi_w^{-1}$ , unitary entropy change for cavity reduction  
 $\Delta C_p$  =  $+\xi_w C_{p,w}$ , slope of the plot  $\Delta H_{den} = f(T)$ , (Class A,  $\Delta C_p > 0$ )  
 $\Delta C_p$  =  $+\xi_w C_{p,w}$ , slope of the plot  $\Delta S_{den} = f(\ln T)$  (Class A,  $\Delta C_p > 0$ )  
 $\Delta C_p$  =  $-\xi_w C_{p,w}$  (Class B,  $\Delta C_p < 0$ )  
 $C_{p,w}$  =  $75.36 \text{ J}\cdot\text{K}^{-1}\cdot\text{mol}^{-1}$ , isobaric heat capacity of liquid water  
 $\Delta G_{mot}$  = motive free energy ( $\Delta G_{mot} = \Delta H_{mot} - T\Delta S_{mot}$ )  
 $\Delta G_{fold}$  = folding free energy ( $\equiv \Delta G_{mot}$ )  
 $\Delta G_{den}$  = denaturation free energy ( $\equiv \Delta G_{mot}$ )  
 $\Delta G_{den}^\circ$  = denaturation free energy at  $c = 0$  denaturant  
 $\Delta G_{unfold}$  = unfolding free energy ( $\equiv \Delta G_{mot}$ )  
 $\Delta G_{therm}$  = thermal free energy = 0 ( $\Delta H_{therm} = T\Delta S_{therm}$ )  
 $K_{den}$  = denaturation equilibrium constant  
CGN = chymotrypsinogen A  
DMSCGN = dimethionine sulfoxide derivative of chymotrypsinogen A  
DPC- $\alpha$ -CT = diphenyl-carbamyl- $\alpha$ -chymotrypsin  
RNase = ribonuclease  
MPD = 2-methyl-2,4-pentanediol  
TMAO = trimethylamine, N-oxide  
 $\xi_w(H)$  =  $\xi_w$  calculated from the enthalpy plot  
 $\xi_w(S)$  =  $\xi_w$  calculated from the entropy plot  
 $K_{for}$  = equilibrium constant for cavity formation  
 $K_{prot}$  = equilibrium constant for protonation  
 $K_{den}$  = denaturation constant =  $K_{for} \cdot K_{prot}$   
HEW = hen egg-white lysozyme  
IC = isothermal calorimetry  
DSC = differential scanning calorimetry  
RNM = random network model  
 $\theta_h$  = hydrogen bond angle  
 $T_{den}$  = denaturation temperature  
 $dV_{for}>0$  = change in volume in cavity formation  
GuHCl = guanidinium hydrochloride  
 $\langle \Delta h_{for} \rangle_A$  =  $-22.2 \pm 0.7 \text{ kJ}\cdot\text{mol}^{-1}\cdot\xi_w^{-1}$ , mean value in Class A  
 $\langle \Delta s_{for} \rangle_A$  =  $-445 \pm 3 \text{ J}\cdot\text{K}^{-1}\cdot\text{mol}^{-1}\cdot\xi_w^{-1}$  mean value in Class A,  
 $\langle \Delta h_{red} \rangle_B$  =  $+23.7 \pm 0.6 \text{ kJ}\cdot\text{mol}^{-1}\cdot\xi_w^{-1}$ , mean value in Class B  
 $\langle \Delta s_{red} \rangle_B$  =  $+432 \pm 4 \text{ J}\cdot\text{K}^{-1}\cdot\text{mol}^{-1}\cdot\xi_w^{-1}$  mean value in Class B

- $Q_{conf}$  = conformational transition N→D  
 $Q_{den}$  = denaturation quotient=[D]/[N]  
 $-\xi_w RT \partial \ln[(W_{III})_T] / \partial (\ln T)$  = change of activity of  $W_{III}$  by temperature

## References

- (1) E. Fiscaro, C. Compari, A. Braibanti, Entropy/enthalpy compensation: hydrophobic effect, micelles and protein complexes, *Phys. Chem. Chem. Phys.* 6 (2004) 4156–4166.
- (2) E. Fiscaro, C. Compari, E. Duce, A. Braibanti, Entropy changes in aqueous solutions of non-polar substances, *J. Solution Chem.* 37 (2008) 487–501.
- (3) E. Fiscaro, C. Compari, E. Duce, M. Biemmi, M. Peroni, A. Braibanti, Thermodynamics of micelle formation in water, hydrophobic processes and surfactant self-assemblies, *Phys. Chem. Chem. Phys.* 10 (2008) 3903–3914.
- (4) E. Fiscaro, C. Compari, and A. Braibanti, Hydrophobic Hydration Processes. General thermodynamic model by thermal equivalent dilution determinations, *Biophysical Chem.* (2010), 151(3), 119-138.
- (5) J. Konicek, I. Wadso, Thermochemical properties of some carboxylic acids, amines, and N-substituted amides in aqueous solution, *Acta Chem. Scand.* 25, (1971) 1541-1951
- (6) H. Frank, F. Franks Structural approach to the solvent power of water for hydrocarbons; urea as a structure breaker. *J. Chem. Phys.* 48 (1968) 4746–4757.
- (7) S. Cabani, G. Conti, A. Martinelli, and E. Matteoli, Thermodynamic properties of organic compounds in aqueous solutions. Apparent molal heat capacities of amines and ethers, *J. Chem. Soc., Farad. Trans. I*, 61 (1973) 2112-2123.
- (8) E. R. Guinto, E. Di Cera, Large heat capacity change in a protein-monovalent cation interaction, *Biochemistry*, 35 (1996) 8800-8804
- (9) R. Lumry, Uses of enthalpy–entropy compensation in protein research, *Biophys. Chem.*, 105 (200) 545–557.
- (10) T. H. Benzinger, Thermodynamics, chemical reactions, and molecular biology, *Nature*, 229 (1971) 100-102
- (11) D. J. Winzor, C. M. Jackson, Interpretation of the temperature dependence of equilibrium and rate constants, *J. Mol. Recognit.* 19 (2006) 389-407
- (12) D. F. Shiao, R. Lumry, J. Fahey, Chymotrypsinogen family of proteins. XI. Heat Capacity changes accompanying reversible thermal unfolding of proteins, *J. Am. Chem. Soc.* 93 (1971) 2024-2035
- (13) R. Lumry, in: A. Braibanti (Ed.), *Bioenergetics and thermodynamics: model systems, Interpretation of Calorimetric Data from Cooperative Systems* Reidel, Dordrecht, 1980, p. 405.
- (14) A. Braibanti, E. Fiscaro, C. Compari, Thermal equivalent dilution, *J. Phys. Chem B*, 102 (1998) 8537–8539.
- (15) W. Pfeil, P.L. Privalov, Thermodynamic investigations of proteins. I. Standard functions for proteins with lysozyme as an example, *Biophys. Chem.*, 4 (1976) 23–32
- (16) P. L. Privalov, Thermodynamic investigations of biological macromolecules, *Pure & Appl. Chem.*, 1976, **47**, 293-304
- (17) J.M. Sturtevant, Biochemical applications of differential scanning calorimetry, *Ann. Rev. Phys. Chem.*, 38 (1987) 463–468.
- (18) P.L. Privalov, S.J. Gill, Stability of protein structure and hydrophobic interaction, *Adv. Protein Chem.*, 39 (1988) 191–234.
- (19) P. Privalov, Thermodynamic problems of protein structure, *Ann. Rev. Biophys. Biophys. Chem.*, 18 (1989) 47–69.
- (20) A. Braibanti, E. Fiscaro, Molecular thermodynamics of the denaturation of lysozyme, *Thermochim. Acta*, 241 (1994) 131-156

- (21) S. N. Timasheff, T. Arakawa, H. Inoue, K. Gekko, M. J. Gorbunoff, J. C. Lee, G. C. Na, E. P. Pittz, V. Prakash, *The role of Solvation in protein stabilization and unfolding* in F. Franks (Ed.) *Biophysics of Water*, J. Wiley (1982) Chichester p. 48
- (22) J.C. Lee, S. N. Timasheff, Partial specific volumes and interactions with solvent components of proteins in guanidine hydrochloride, *Biochemistry*, 13 (1974) 257-265.
- (23) S. N. Timasheff, Water as ligand: Preferential binding and exclusion of denaturants in protein unfolding, *Biochemistry*, 31 (1992) 9857-9864.
- (24) D. Poland, Protein Denaturant Binding Polynomials, *J. Protein Chem.* 21 (2002) 479-487
- (25) J. A. Schellman, Fifty Years of solvent denaturation, *Biophys. Chem.* 96 (2002) 91-101.
- (26) S. Lapaje, C. Tanford, Proteins as random coils. IV. Osmotic pressures, second virial coefficients, and unperturbed dimensions in 6M guanidine hydrochloride, *J. Am. Chem. Soc.* 89 (1967) 5030-5033
- (27) Y. Qu, C. L. Bolen, D. W. Bolen, Osmolyte-driven contraction of a random coil protein, *Proc. Nat. Acad. Sci., USA*, 95 (1998) 9268-9273
- (28) I. Baskanov, D. W. Bolen, Forcing thermodynamically unfolded proteins to fold. *J. Biol. Chem.* 273 (1998) 4831-4834
- (29) K. Anand, D. Pal and R. Hilgenfeld, An overview on 2-methyl-2,4-pentanediol in crystallization and in crystals of biological macromolecules, *Acta Cryst.* (2002). D58, 1722-1728
- (30) E. A. Galinski, M. Stein, B. Amendt, M. Kinder, The Kosmotropic (Structure-Forming) Effect of Compensatory Solutes, *Comparative Biochemistry and Physiology Part A: Physiology*, 117, (1997), 357-365.
- (31) R. Koynova, J. Brankov and B. Tenchov Modulation of lipid phase behaviour by kosmotropic and chaotropic solutes, *European Biophysics Journal*, 25 (1997) 261-274
- (32) D. B. Wetlaufer, S. K. Malok, L. Stoller, R.L. Coffin, Nonpolar group participation in the denaturation of proteins by urea and guanidinium salts. Model compound studies, *J. Am. Chem. Soc.* 86 (1964), 508-514
- (33) D. T. Haynie (*Biological Thermodynamics*, Cambridge Univ Press, Cambridge, (2001) p.169
- (34) N. Pace, C. Tanford, Thermodynamics of the unfolding of beta-lactoglobulin A in aqueous urea solutions between 5 and 55 degrees, *Biochemistry*, 7 (1968) 198-208
- (35) F. Vanzi, B. Madan, K. Sharp, Effect of the Protein Denaturants Urea and Guanidinium on Water Structure: a Structural and Thermodynamic Study, *J. Am. Chem. Soc.* 120 (1998) 10748-10753
- (36) K.A. Sharp, B. Madan, Hydrophobic Effect, Water Structure, and Heat Capacity Changes, *J. Phys. Chem.* 101 (1997) 4343-4348.
- (37) B. Widom, P. Bhimalapuram, K. Koga. The hydrophobic effect, *Phys. Chem. Chem. Phys.*, 5 (2003) 3085-3093
- (38) P. J. Rossky, Protein Denaturation by urea: Slash and bond, *Proc. Nat. Acad. Science U.S.A. PNAS*, 105 (2008) 16825-16826
- (39) D. Chandler, Insight Review: interfaces and the driving force of hydrophobic assembly, *Nature*, 437 (2005) 640-647
- (40) S. Rajamani, T.M. Truskett, S. Garde, Hydrophobic hydration from small to large length scales: Understanding and manipulating the crossover, *PNAS*, 102 (2005) 9475-9480
- (41) K. Lum, D. Chandler, J. D. Weeks, Hydrophobicity at Small and Large Length Scales, *J. Phys. Chem. B*, 103 (1999) 4570-4577
- (42) V.V. Yaminsky, E. A. Vogler, Hydrophobic Hydration, *Curr. Opinions in Colloid & Interface Science*, 6 (2001) 342-349
- (43) H. S. Frank, M. W. Evans Free volume and entropy in condensed systems. III. Entropy in binary liquid mixtures; partial molal entropy in dilute solutions; structure and thermodynamics in aqueous electrolytes, 13 (1945) 507-532

- (44) G. Nemethy, H.A. Scheraga, Structure of water and hydrophobic bonding in proteins. I. A model for the thermodynamic properties of liquid water, *J. Chem. Phys.*, 36 (1962) 3382-3400
- (45) G. Graziano, A van der Waals approach to the entropy convergence phenomenon, *Phys. Chem. Chem. Phys.*, 6 (2004) 406-441
- (46) Y- D. Linney, R. Edelman. I. Kusner, R. Kisillak, S. Srebic, Water structure effect of sugar stereochemistry and its impact on protein thermal stability, *Frontiers in Water Biophysics*, May 23-26 2010, Trieste

ACCEPTED MANUSCRIPT



Table 1. Equations representing the cumulative curves at pH=2.

PROTEIN	Equation	Points	R <sup>2</sup>
CGN	$\log K_{den} = -37.458 (1/T)^3 + 388.76 (1/T)^2 - 1355.8 (1/T) + 1584.6$	147	0.9985
DMSCGN	$\log K_{den} = -0.9549 (1/T)^3 + 33.161 (1/T)^2 - 198.21 (1/T) + 327.86$	301	0.9947
DPCT $\alpha$	$\log K_{den} = -14.750 (1/T)^3 + 190.65 (1/T)^2 - 793.71 (1/T) + 1072.8$	141	0.9982
RNase	$\log K_{den} = -6.4058 (1/T)^3 + 76.173 (1/T)^2 - 307.71 (1/T) + 416.62$	92	0.9996

Table 2. Denaturation Enthalpy and Entropy as sum of motive and thermal components.

compd	$\Delta H_{den} = \Delta H_{mot} + \Delta H_{therm}$	$\Delta S_{den} = \Delta S_{mot} + \Delta S_{therm}$
	$\Delta H_{mot}$ $\xi_w(H) C_{p,w}T$	$\Delta S_{mot}$ $\xi_w(S) C_{p,w} \ln T$
	$\text{kJ} \cdot \text{mol}^{-1}$ $\text{kJ} \cdot \text{mol}^{-1}$	$\text{J} \cdot \text{K}^{-1} \cdot \text{mol}^{-1}$ $\text{J} \cdot \text{K}^{-1} \cdot \text{mol}^{-1}$
DMSCGN	-2823 $132.2 C_{p,w}T$	-56615 $132.6 C_{p,w} \ln T$
CGN	-4137 $191.0 C_{p,w}T$	-81181 $189.7 C_{p,w} \ln T$
DPCT- $\alpha$	-5173 $241.6 C_{p,w}T$	-101958 $240.6 C_{p,w} \ln T$
R Nase	-1023 $56.6 C_{p,w}T$	-24088 $37.5 C_{p,w} \ln T$

Table 3. Motive Functions: cavity formation and intra-chain interactions.

Enthalpy	Entropy
$\Delta H_{mot} = \Delta H_0^{(\xi_w=0)} + \xi_w \Delta h_{for}$	$\Delta S_{mot} = \Delta S_0^{(\xi_w=0)} + \xi_w \Delta s_{for}$
$\Delta H_{mot} = +205.05 - 22.5 \xi_w$	$\Delta S_{mot} = -59.7 - 424.2 \xi_w$

Table 4. Motive parts of the thermodynamic functions for protein denaturation.

Protein	$\Delta H_0$	$T \Delta S_0$	$\Delta G_0 (298/K)$
	$\text{kJ} \cdot \text{mol}^{-1}$	$\text{kJ} \cdot \text{mol}^{-1}$	$\text{kJ} \cdot \text{mol}^{-1}$
DMSCGN	-2823	$T \cdot 56.62$	14050
CGN	-4137	$T \cdot 81.18$	20055
DPCT-a	-5173	$T \cdot 101.96$	25096
R Nase	-1023	$T \cdot 24.09$	6156

Table 5. Thermodynamic functions calculated from the van't Hoff plot of  $\Delta \log K$  (\*).

Protein	Equation	$R^2$	$\Delta H_{prot}$	$(1/3)\Delta H_{prot}$	$\Delta S_{prot}$	$(1/3)\Delta S_{prot}$
			$\text{kJ}\cdot\text{mol}^{-1}$	$\text{kJ}\cdot\text{mol}^{-1}$	$\text{J}\cdot\text{K}^{-1}\cdot\text{mol}^{-1}$	$\text{J}\cdot\text{K}^{-1}\cdot\text{mol}^{-1}$
CGN	$Y = 3.0716(1/T) - 26.188$	0.9153	-51.41	-17.1	-120.3	-40.1
DMSCGN	$Y = 2.6851(1/T) - 6.2841$	0.9611	-58.81	-19.6	-501.4	-167.1
DCPT	$Y = -6187(1/T) - 19.764$	0.9156	+50.1	+16.7	-378.8	-126.2
RNase	$Y = -2.7027(1/T) + 32.25$	0.9825	+51.7	+27.2	+617.4	+205.8

(\*) Division by 3 (cfr. power  $\langle x \rangle = 3.04 \pm 0.08$  in Table B.1) to refer to a one-site reaction

Table 6. Dehydration numbers,  $\xi_w$  from calorimetry in different types of lysozyme.

Type	slope	$\xi_w$	$\Delta H^\circ$	$T_{ad}$ (!)
	$\text{J}\cdot\text{mol}^{-1}\cdot\text{K}^{-1}$		$\text{kJ}\cdot\text{mol}^{-1}$	K
HEW	6701	88.9	-1764.8	263.4
wild T4	9199	122	-2463.4	267.8
T157A(T4)	9903	131.4	-2701.7	272.8
R96H (T4)	10539	139.8	-2896.2	274.8

(!)  $T_{ad}$  is the temperature where  $\Delta H_{app} = 0$  (adiabatic)

Table 7. Enthalpy and entropy functions in corresponding processes( $^\circ$ ).

Process	Class	$\Delta H_0^{(\xi_w=0)}$	$\Delta h_w$	$\Delta S_0^{(\xi_w=0)}$	$\Delta s_w$
		$\text{kJ}\cdot\text{mol}^{-1}$	$\text{kJ}\cdot\text{mol}^{-1}\cdot\xi_w^{-1}$	$\text{J}\cdot\text{K}^{-1}\cdot\text{mol}^{-1}$	$\text{J}\cdot\text{K}^{-1}\cdot\text{mol}^{-1}\cdot\xi_w^{-1}$
Protein Denat. (van't Hoff)	A	+211.82	-22.5	+415.8	-424.2
Protein Denat. (calorim.)	A	+221.3	-22.6	-	-
Protein Folding	B	-211.82	+22.5	-415.8	+424.2
Micelle formation	B	-3.97	+23.13	+10.2	+428
Non-polar gas solub.	A	-17.7	-21.6	-86.4	-445

( $^\circ$ )  $\Delta h_w$  and  $\Delta s_w$  indicate general unitary thermodynamic functions of either Class, i.e.  $\Delta h_w$  and  $\Delta s_w$  indicate  $\Delta h_{for}$  and  $\Delta s_{for}$ , respectively, in Class A and  $\Delta h_{red}$  and  $\Delta s_{red}$ , respectively, in Class B.

Table 8. Process of thermal denaturation.

<b>N</b>	<b>Exper.</b>	<b>Thermodynamic Function</b>	<b>Physico-Chemical Process</b>
<b>0</b>	<b>Rest</b>	$\Delta S_{red} = +\xi_w 424 \text{ J}\cdot\text{K}^{-1}\cdot\text{mol}^{-1}$	<b>Native Protein (Folded)</b>
<b>1</b>	<b>Heat Supply Start</b>	$dQ/T = dS_{therm}$ $dS_{therm} \rightarrow dV_{for} > 0$ $dV_{for} \rightarrow dS_{for}$ $dS_{for} = -424 \text{ J}\cdot\text{K}^{-1}\cdot\text{mol}^{-1} d\xi_w$ $\Delta S_{red} + dS_{for}$	<b><math>W_{III} + \text{Cavity Formation}</math></b> <b>Initial Break of Hydroph. Bonds</b> <b>Initial Cancelling of Entropy <math>\Delta S_{red}</math></b>
<b>2</b>	<b>Scan</b>	$\int_{T_1}^{T_2} C_{p,app} dT = Q_{cal}$ $Q_{cal} \rightarrow \int dS_{for} = \Delta S_{for}$ $\Delta S_{for} = -\xi_w 424 \text{ J}\cdot\text{K}^{-1}\cdot\text{mol}^{-1}$	<b>Cavity <math>\longrightarrow</math> Forming</b> <b>Entropy <math>\Delta S_{red} \longrightarrow</math> Cancelling</b> <b>Hydroph. Bonds <math>\rightarrow</math> Breaking</b>
<b>3</b>	<b>Final</b>	$\Delta S_{red} + \Delta S_{for} =$ $+ \xi_w 424 - \xi_w 424 = 0$	<b>Entropy <math>\Delta S_{red} \longrightarrow</math> Cancelled</b> <b>Hydroph. Bonds <math>\longrightarrow</math> Broken</b> <b>Protein <math>\longrightarrow</math> Denatured (Unfolded)</b>

Table 9. Denaturants and stabilising molecules for proteins.

Denaturant	Stabilizing
6 M GdnHCl	Sucrose
Urea	2-methyl-2,4-pentanediol (MPD)
.2-Chloroethanol 40%	Glycine-betaine
Methoxyethanol 40%	Na <sub>2</sub> SO <sub>4</sub>
	Glycerol
	trimethylamineN- oxide (TMAO)

Table 10. Denaturation of  $\beta$ -lactoglobuline. Change of number  $\xi_w$  at high urea concentration.

Urea conc.	4.42 M	5.09 M	5.59 M
$\xi_w$	118..2	117.7	92.1
$\Delta\xi_w$	----	-0.47	-25.6

Table 11. Curvatures ( $\xi_w$ ) of hydrocarbons solubility in water, and in concentrated urea solution.

<i>Compound</i>	Water	Urea 4M
	$\xi_w$	$\xi_w$
methane	2.6	0.47
ethane	3.5	1.22
buthane	4.72	3.54

Table B.1. Relationships between  $\Delta(\log[H^+]^x)$  and  $\Delta(\text{pH})$ .  
 $\langle x \rangle = 3.04 \pm 0.08$ 

<i>Compound</i>	<i>Equation</i>		<i>x</i>
DMSCGN	$y = 3.16 \Delta\text{pH}$	+0.02	3
CGN	$y = 2.97 \Delta\text{pH}$	+0.06	3
DPC- $\alpha$ -CT	$y = 2.99 \Delta\text{pH}$	+0.09	3
Rnase	$y = 3.03 \Delta\text{pH}$	+0.02	3

Fig. 1. A unique reaction, involving water, either direct (left, Class A)) or inverse (right, Class B) takes place in every hydrophobic hydration process:

- Unfolding (Class A): transformation  $\mathbf{A}(-\xi_w W_I \rightarrow \xi_w W_{II} + \xi_w W_{III} + \text{cavity})$ , with melting of  $\xi_w$  water molecules  $W_{III}$ .
- Folding (Class B): transformation  $\mathbf{B}(-\xi_w W_{III} - \xi_w W_{II} \rightarrow \xi_w W_I - \text{cavity})$ , with condensation of  $\xi_w$  water molecules  $W_{III}$ .

Cavity expansion or reduction ( $\pm \Delta W_I$ , in grey) is proportional to  $\xi_w$ . Note, please, that the sum of white and grey areas at the bottom equals the sum of the separated white areas at the top.

Figure 1

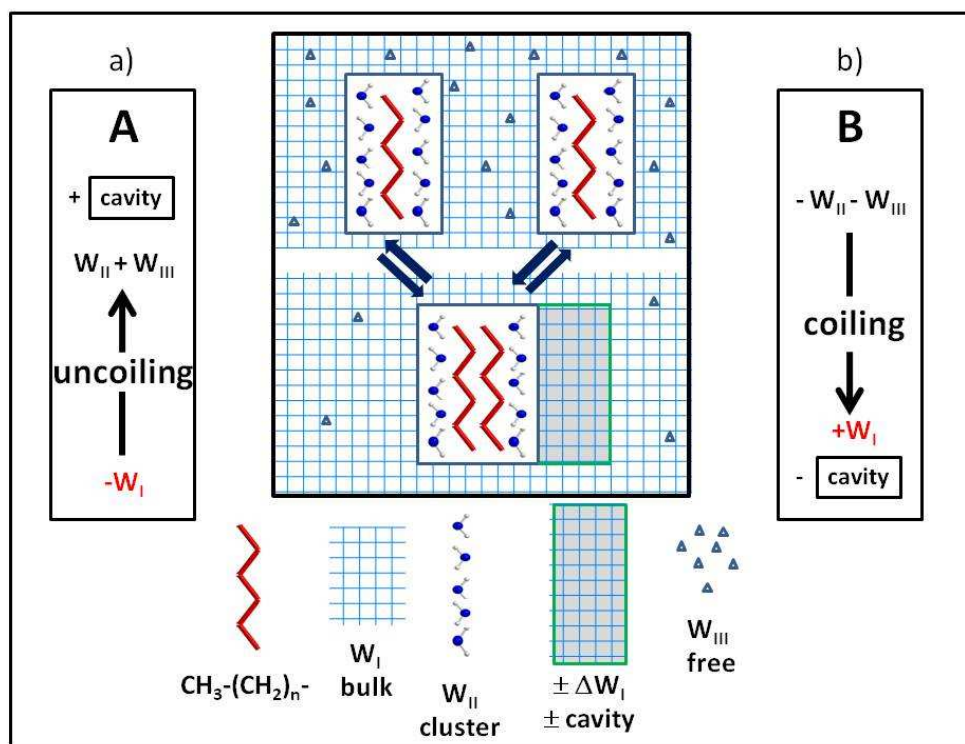


Fig. 2. Examples of free energy plots  $(-\Delta G^0)/RT = \ln K = f(1/T)$  in hydrophobic hydration processes  
**Figure 2**

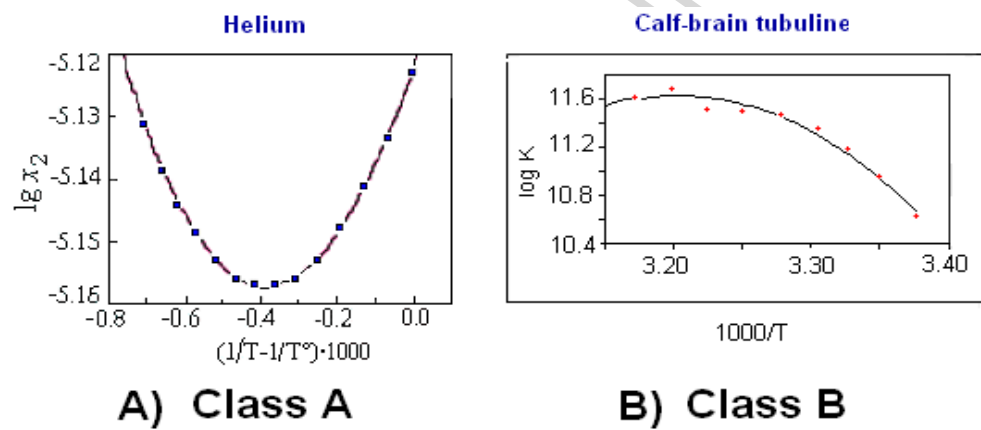


Fig.3. Mechanism of unfolding of a protein.

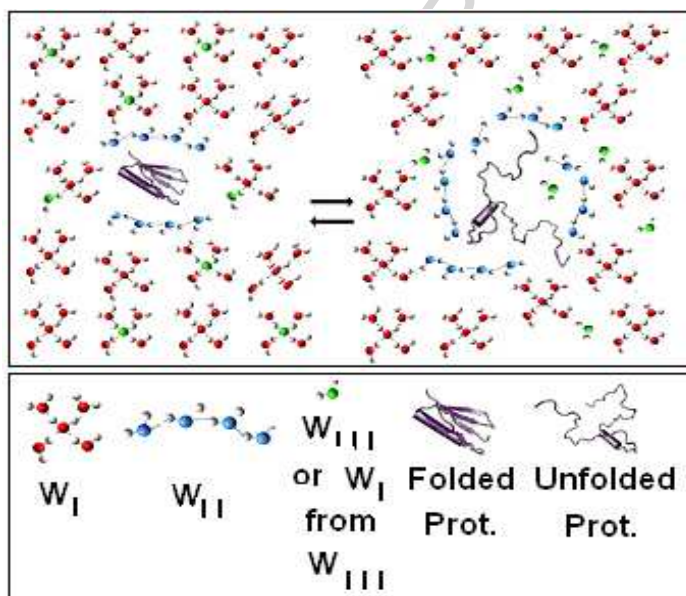
**Figure 3**

Fig.4. Cumulative curve of  $\log K_{den}$  for DMSCGN (dimethionine sulfoxide derivative of chymotrypsinogen) with all the branches displaced to pH=2. Parallel displacement to pH = 0 brings the whole curve in the positive range of  $\log K_{den}$  ( $\Delta G_{den} < 0$ ) where the denatured state is stable

## Figure 4

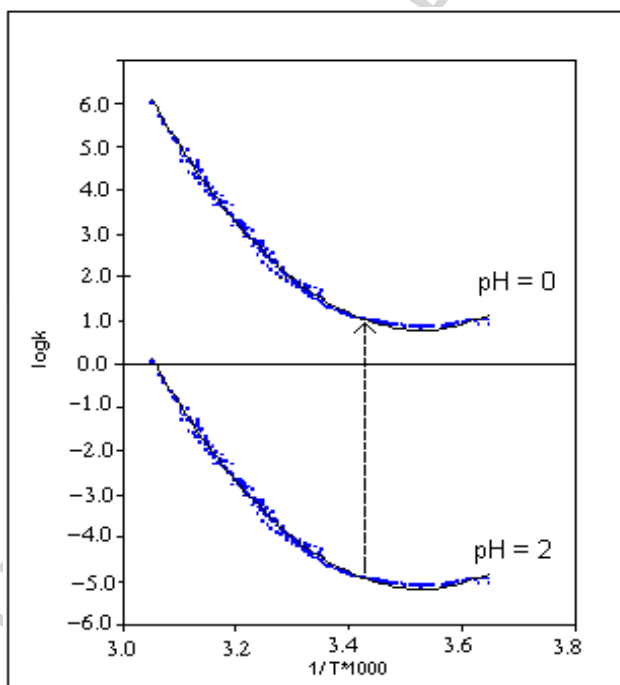




Fig. 5. Example of plot  $\Delta H_{den} = f(T)$  (DMSCGN, dimethionine sulfoxide derivative of chymotrypsinogen)

### Figure 5

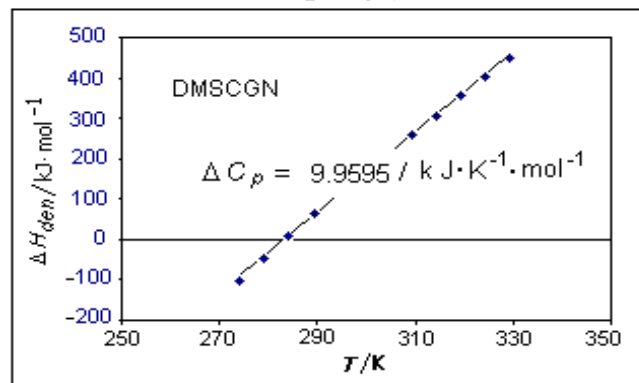


Fig.6. Example of entropy plot. (DMSCGN, dimethionine sulfoxide derivative of chymotrypsinogen)

**Figure 6**

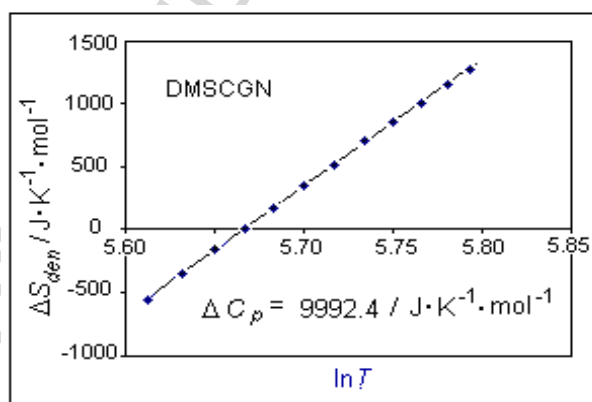


Fig. 7. Motive parts of enthalpy, entropy and free energy for protein denaturation ( $\Delta H_{mot} = -2823 \text{ kJ}\cdot\text{mol}^{-1}$ )

## Figure 7

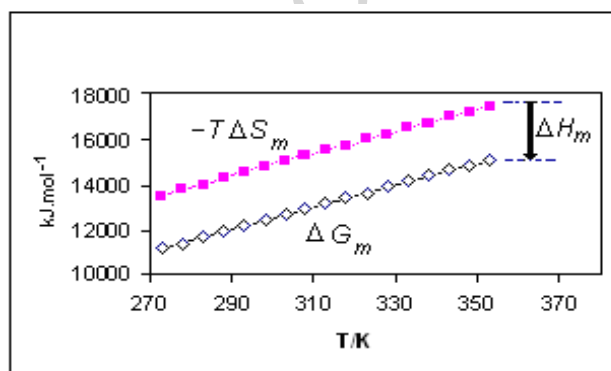


Fig. 8. Calculated free energies in protein denaturation

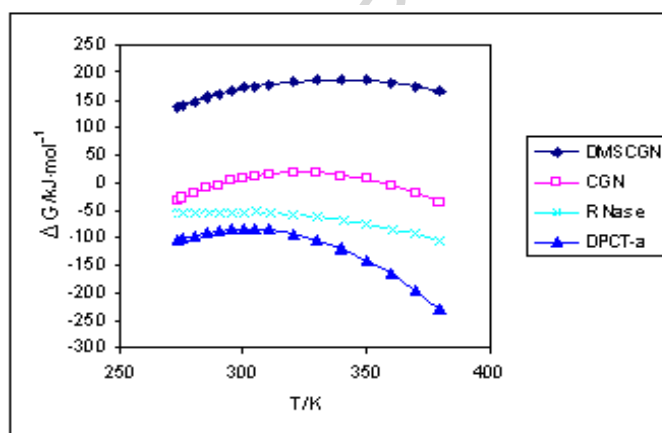
**Figure 8**

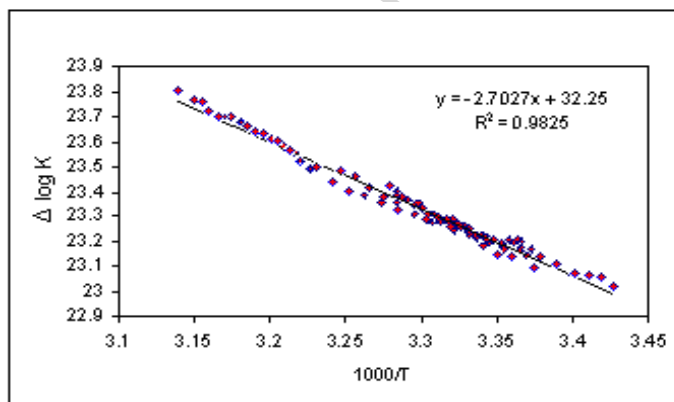
Fig. 9. Van't Hoff plot of  $\Delta \log K$  for RNase.**Figure 9**

Fig. 10. Dependence of enthalpy on the temperature  $T_{den}$  for a wild type of lysozyme from bacteriophage T4 and its T157A mutant.

**Figure 10**

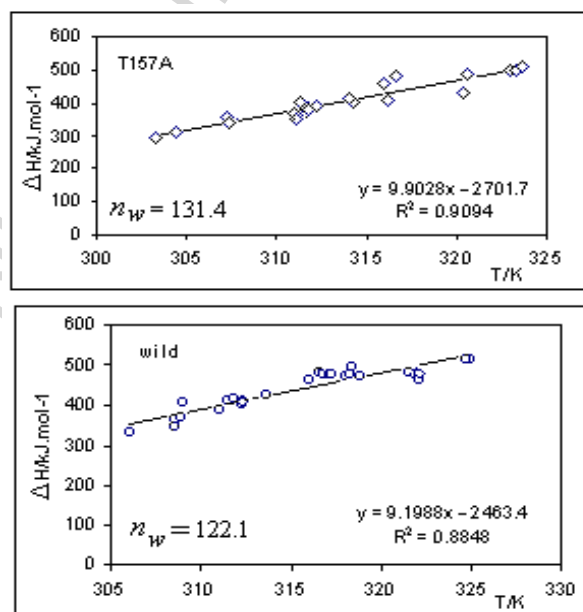


Fig. 11. a) Native folded state, stable ( $\Delta G_{fold} < 0$ ) because entropy driven ( $\Delta S_{red} \gg 0$ )  
 b) Thermal denaturation at temperature  $T_d$ : after heat supply, melting of water  $W_{III}$  has created a cavity, entropy consuming.  $\Delta S_{for} \ll 0$  compensates for  $\Delta S_{red} \gg 0$ , leading to stable denatured state (unfolding) with  $\Delta G_{unfold} < 0$ .

**Figure 11**

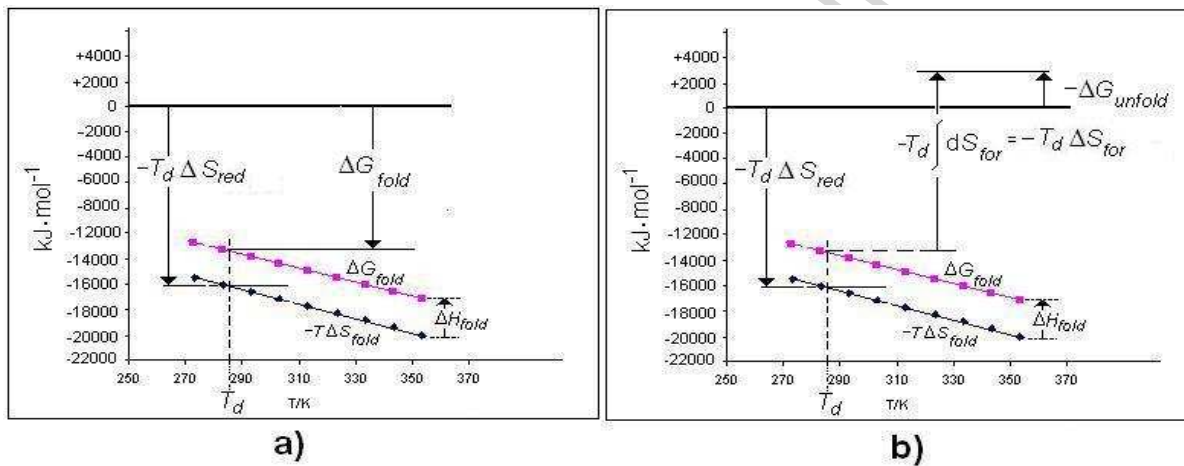


Fig. 12. a) Lysozyme. The slope is constant (*i.e.*  $\Delta C_p$  is constant) whatever thermal or chemical denaturation and whatever the experimental method (Data from Privalov [16]).

**Figure 12**

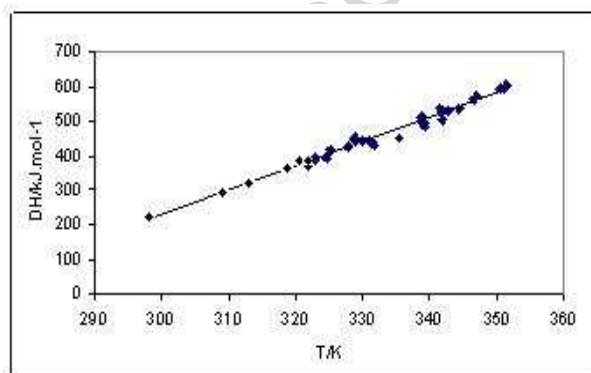




Fig. 13. The action of denaturant displaces the equilibrium in water toward formation of cavity with negative entropy production, that cancels the positive entropy gain of folding.

**Figure 13**

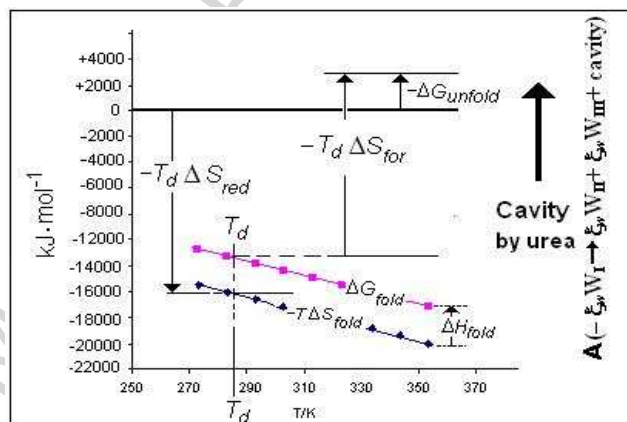


Fig. 14. Solubility of butane in aqueous solutions of urea and of guanidinium hydrochloride

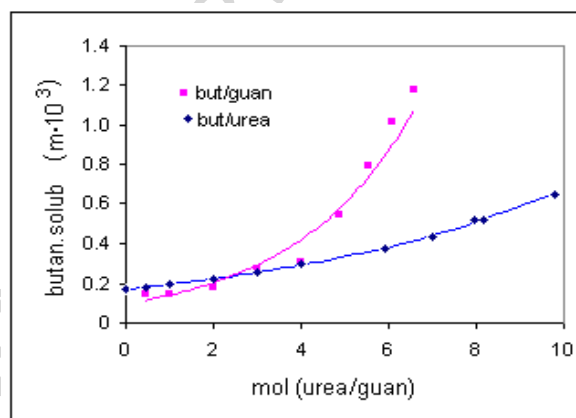
**Figure 14**

Fig. 15. Hydrogen bonding of water to urea (A) is less efficient than to guanidinium ion (B).  
Salting-in effect is lower in urea solutions than in guanidinium solutions

**Figure 15**

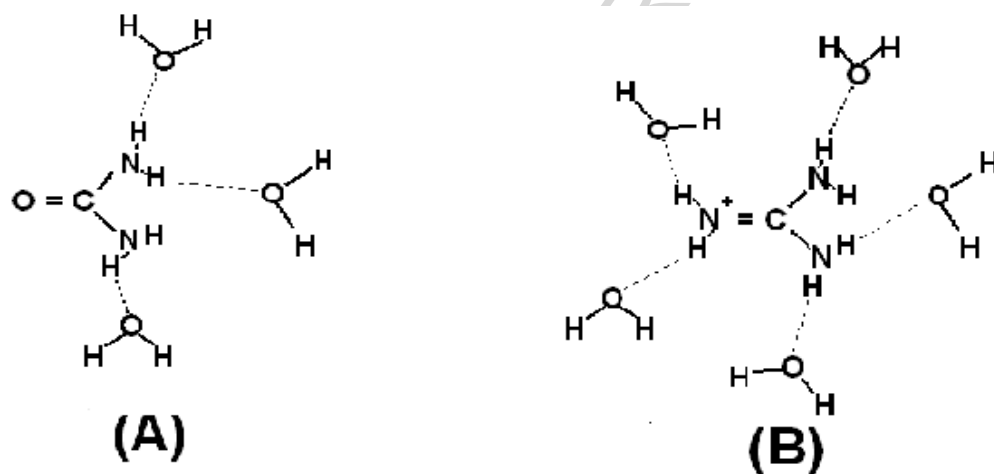


Fig. 16.  $\beta$ -globuline: the curves are becoming smoother at high concentration of urea, i.e.  $\Delta C_p$  is sharply decreasing when urea concentration is large enough (From Ref. [34])

**Figure 16**

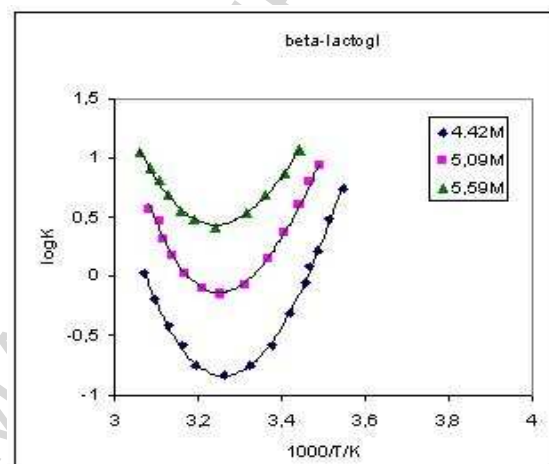


Fig. 17. Solubility of hydrocarbons in water and urea at different temperatures

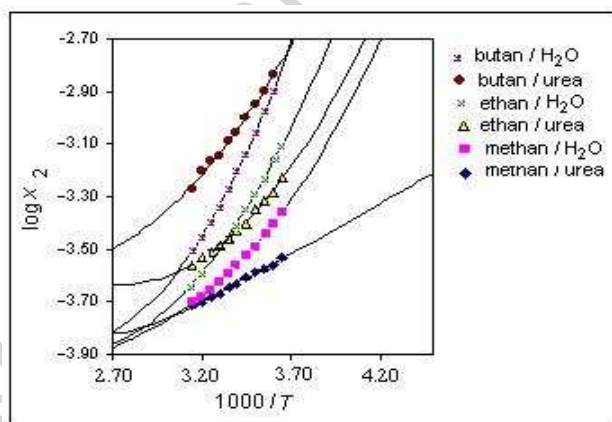
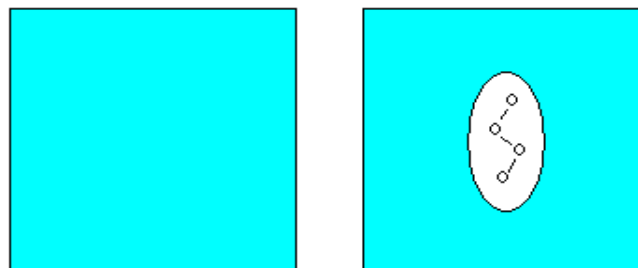
**Figure 17**

Fig.18. a) Small molecule: the cavity surrounds the whole molecule; the trapped gas molecules lose their configurational entropy ( $\Delta S_0^{(\xi_w=0)} = -86.4 \text{ J}\cdot\text{K}^{-1}\cdot\text{mol}^{-1}$ )

b) Macromolecule: the cavity surrounds only the unfolded chains; the core C remains almost invariant but the solvent volume is reduced and the solute becomes more concentrated ( $\Delta S_0^{(\xi_w=0)} = -59.7 \text{ J}\cdot\text{K}^{-1}\cdot\text{mol}^{-1}$ ).

**Figure 18**

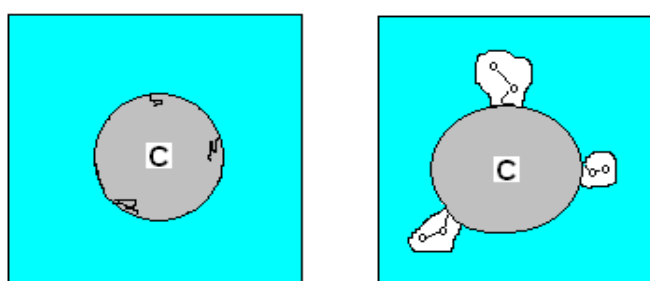
**a) solubility of small molecule**



1) solvent

2) solution

**b) unfolding in macromolecule**



1) folded

2) unfolded .

Fig. B.1. Determination of denaturation free energy at different pH and different temperatures. The curve at each pH is the branch  $br_j$  (pH=3, or 2.4,...) with origin at  $O_j$ .

**Figure B1**

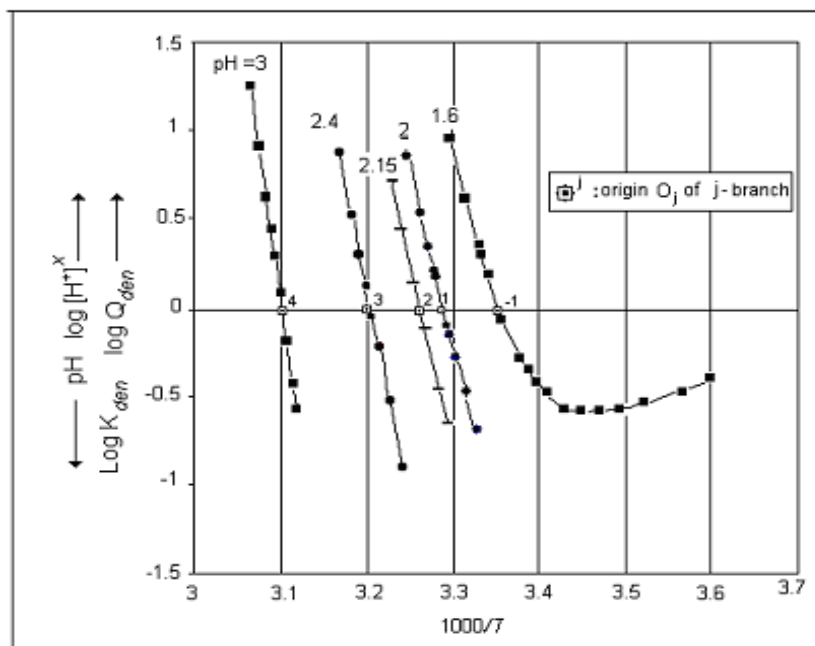


Fig. B 2. Sections of the cumulative denaturation curve can be moved to the range of  $\log Q$  around 0 by increasing pH. The shape of the curve is invariant because  $\Delta C_p$  is constant.

## Figure B2

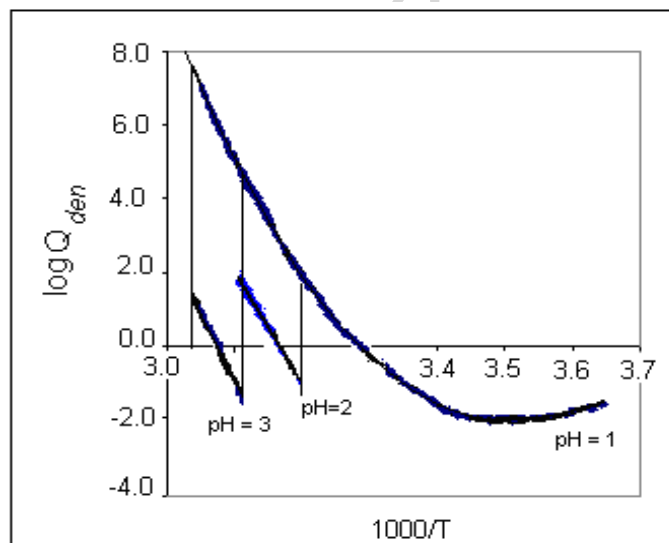




Fig. B.3. The cumulative curve obtained by displacement of each branch to pH = 0. At the right hand, the scale for displacement to pH =2: the curve is partially in the negative field of  $\log Q_{den}$

**Figure B3**

